BIOGRAPHICAL SKETCH

Dr. Smedes has been a research geologist for the United States Geological Survey since 1953. Prior to that he served in the U.S. Navy during World War II and taught in the Geology Department at Kansas State University.

His career has included geologic and mineral deposits studies in Oregon, Montana, and Wyoming where he specialized in the study of volcanic and plutonic igneous rocks. He coordinated and engaged in studies of remote sensing as part of his volcanologic studies in Yellowstone National Park, and is now responsible for research in geologic mapping techniques.

He received a B.S. degree with honors and a Ph.D degree in Geology at the University of Washington, with minors in Physics and Chemistry. He is a Fellow of the Geological Society of America and the Mineralogical Society of America; a Corporate Member of the American Society of Photogrammetry; and a Member of the Colorado Scientific Society and the Society of Sigma Xi.

Dr. Smedes' biography is listed in American Men of Science, Who's Who (South and Southwest), and the Dictionary of International Biography. He has published numerous maps and technical reports in his fields of specialization and has been selected as author-editor of the section on image enhancement of the new Manual of Remote Sensing (in preparation).

AUTOMATIC COMPUTER MAPPING OF TERRAIN*

by

Harry W. Smedes
U.S. Geological Survey
Denver, Colorado

ABSTRACT

Computer processing of 17 wavelength bands of visible, reflective infrared, and thermal infrared scanner spectrometer data, and of three wavelength bands derived from color aerial film has resulted in successful automatic computer mapping of eight or more terrain classes in a Yellowstone National Park test site.

The tests involved: 1) supervised and 2) non-supervised computer programs; 3) special preprocessing of the scanner data to reduce computer processing time and cost, and improve the accuracy; and 4) studies of the effectiveness of the proposed Earth Resources Technology Satellite (ERTS) data channels in the automatic mapping of the same terrain, based on simulations, using the same set of scanner data.

The following terrain classes have been mapped with greater than 80 percent accuracy in a 12-square-mile area with 1,800 feet of relief: 1) bedrock exposures, 2) vegetated rock rubble, 3) talus, 4) glacial kame meadow, 5) glacial till meadow, 6) forest, 7) bog, and 8) water. In addition shadows of clouds and cliffs are depicted, but were greatly reduced by using preprocessing techniques.

AUTOMATIC COMPUTER MAPPING OF TERRAIN*

Harry W. Smedes

PURPOSE AND SCOPE

For several years now there have been discussions and expressions of concern about the need to examine vast areas of the earth's surface, the advantages of high-altitude aircraft and satellite-borne remote sensors to gather the needed data, and at the same time concern about the immense quantity of data that is needed and would become available. Handling these data will require automatic processing by computer--not to make the final and only decisions of classification, but to perform one or more of the following three basically different tasks:

1) to perform the first-approximation rough interpreting, calling attention to special places that warrant examination by a human interpreter;

2) to enable us to extend our interpretation far beyond the range of human vision into the reflective infrared and thermal infrared, at the same time combining and integrating the data from many different parts of this expanded spectrum--something which cannot be done from the study of any single image; and

3) to enable us to extract additional information by either amplifying very small differences in radiance which are on or even below the limit of visual recognition, or by portraying broad ranges in radiance uniformily as a single value in order to determine or clarify relations previously obscured by mottled radiance.

For some of these operations a human can do a better job of interpreting, but the computer can do it faster. In this case, computer processing is largely a matter of data compression. However, some others of these operations cannot be done directly by a human interpreting some image or images. In these cases the computer processing enables man to extend his capability and perform tasks not otherwise possible.

It is for these reasons that the U.S. Geological Survey engaged in this study of automatic data processing by computer, that includes:

A. Testing the suitability of existing sensors and computer software;

B. Determining how many and what kinds of natural and manmade terrain classes can be satisfactorily classified in this particular climatic region;

C. Simulating the spectral response of the proposed Earth Resources Technology Satellite (ERTS) sensors.

This report summarizes the current status of studies of computer processing of airborne multispectral data and color photographs, the success of automatic recognition and mapping of the distribution of eight or more different terrain classes, and the effectiveness of the proposed ERTS data channels in the automatic recognition and mapping of the same terrain classes based on simulations, using the same set of scanner data.

This study involves the data from one flight over a test area of about 12 square miles in a region of moderate relief (1,800 feet) comprising a wide variety of terrain types (Figures 1 and 2).

The data were acquired and processed in analog and digital form by the Institute of Science and Technology of the University of Michigan; and were processed in digital form by the Laboratory for Applications in Remote Sensing (LARS) at Purdue University; the Center for Research (CRES) at the University of Kansas; and EG&G, Inc. of Bedford, Massachusetts. The project also involved limited studies of spatial pattern recognition using optical lasers, and image enhancement by electronic and optical methods, but these studies are not described in this report.

COLLECTION OF THE DATA

A multispectral survey was made of selected test areas in Yellowstone National Park during flights by the University of Michigan in September 1967, on a NASA-sponsored contract to the U.S. Geological Survey.

The University of Michigan 12-channel scanner-spectrometer in the 0.4 to 1.0μm range (Table I) provided the principal data for the computer processing described in this report. In addition, two scanner systems recorded a total of five channels of reflective and thermal infrared data in the region from 1.0 to 14μm.

Photographs taken at the same time the scanner data were acquired provide important supplements to the control data. These photographs consist of color, color infrared, black and white panchromatic, and black and white infrared film on board the aircraft, and color film from stations on the ground. Special computer processing was performed on some of the color aerial film for comparison with scanner data.

A simplified diagram of the Michigan scanner-spectrometer is shown in Figure 3. As the aircraft flies over the test area, the ground surface is scanned in overlapping strips by successive sweeps as a mirror is rotated at about 3,600 rpm. The radiant energy from the earth's surface is reflected off the rotating mirror and focused, by other mirrors (M, Figure 3) onto the slit of a prism spectrometer, thus refracting the rays into a wavelength spectrum.

Fiber optics placed at appropriate places lead to photomultiplier tubes which measure the amount of radiant energy received in each of 12 overlapping bands or channels of this spectrum from 0.4 to 1.0μm (visible violet to reflective infrared). This energy, which is now a voltage, is fed to a multitrack tape recorder where each of the 12 channels is recorded as a separate synchronized signal on magnetic tape. Similar, separate scanners recorded the infrared part of the spectrum from 1 to 14μm (see Table I).

Table I. Wavelength bands of University of Michigan multispectral system.

Channel number	Wavelength band μm	Channel number	Wavelength band μm
		SCANNER NO. 1	
1	0.40-0.44	7	0.55-0.58
2	.44- .46	8	.58- .62
3	.46- .48	9	.62- .66
4	.48- .50	10	.66- .72
5	.50- .52	11	.72- .80
6	.52- .55	12	.80-1.00
		SCANNER NO. 2	
1	1.0 -1.4	3	3.0 - 4.1
2	2.0 -2.6	4	*4.5 - 5.5
		SCANNER NO. 3	
---	*8.0-14.0		

*Denotes thermal infrared channels; others are reflective

TERRAIN CLASSES MAPPED

The eight terrain classes discussed on the following pages were selected arbitrarily during field study and the early part of computer processing. They were selected not on the basis of composition or genesis, as we traditionally do in the course of geologic mapping, but on the basis of their overall surface color and radiance (brightness) inasmuch as that is what the sensor was recording.

For example, geologists are more interested in the areal distribution of a sand and gravel unit, such as glacial till, than in the distribution of forest. Conventional maps would show the extent of till regardless of whether it was the site of a meadow or was covered with dense forest. The terrain classes of this study necessarily show the unforested till as one class (till) and the forested till as a different class (forest). In fact, all forested terrain, regardless of underlying rock or soil unit, is shown as a single class (forest).

Initial processing disclosed that at least 13 classes could be separated. Several of these were subunits which have been combined to make the display shown in Figure 25. The following is a brief description of the nine classes (including shadows) mapped.

1. BEDROCK EXPOSURES

   This class (Figure 4) consists of bare bedrock exposed by glacial and stream erosion and mantled by minor amounts of loose rubble. These are unvegetated except for lichens and sparse tufts of dry grass, and have high reflectance in nearly all channels.

2. TALUS

   This class includes blockfields, talus, and talus flows of basalt lava flows, volcanic tuff, and gneiss, formed by frost-riving and solifluction from outcrops. These are blocky and well-drained deposits; trees are widely spaced or absent (Figure 5). Blocks generally are covered with dark-gray lichens (Figure 6). The blocks range from a few centimeters to about 1 meter in diameter; most are larger than 10 centimeters. The slopes range widely, from 35°-45° at the head, to 5° or less at the toe. In places, a basin or trough lies just inside the distal margin of talus flows.

3. VEGETATED ROCK RUBBLE

   This class consists of locally derived angular rubble, frost-riven from basalt lavas, volcanic tuff and breccia, and gneiss. Grasses, lichens, evergreen seedlings, and mosses now cover more than three-fourths of the surface underlain by this debris (Figures 7 and 8). Blocks range in diameter from less than 1 centimeter to about 1 meter, and occur on slopes of from 0° to about 25°.

4. GLACIAL KAME MEADOW

   These are meadows underlain by sand and gravel, and mantled by sandy silt (Figures 9 and 10). The deposits are well-drained and are vegetated by grass and sagebrush. About one-fourth of the area of this class is exposed mineral soil. Deer and elk manure locally covers as much as one-fourth the surface area.

5. GLACIAL TILL MEADOW

   This class consists of meadow areas underlain by glacial till. These are grassland and sagebrush areas (largely dormant at time of flight) with mineral soil exposed over about one-fifth of the area (Figures 11, 12, and 13). Mineral soil consists of mixtures of silty to bouldery debris. Deer and elk manure locally is abundant in these meadows.

6. FOREST

   Depicted here are Douglas Fir and lodgepole forest (see Figure 5). Local clusters of deciduous trees were recognized separately, but combined with evergreens in the displays.

7. BOG

   These are moist areas supporting tall lush growth of sedges and grasses. Bogs are rather abundant because of glacial scour and derangement of drainages.

8.   WATER

The Yellowstone River and Floating Island Lake are present in the test area. Phantom Lake was dry at the time of flight, and was considered therefore as bog rather than water.

9.   SHADOWS

Cloud shadows are near west and south-central margins of the test area, and deep shade occurs at base of north-facing cliffs and along north edge of forest areas.

DATA PROCESSING BY ANALOG COMPUTER

This section of the report, dealing with analog processing, was conducted at the University of Michigan.

Any given channel of magnetic tape data can be reproduced by photographing a cathode-ray tube video (C-scope) presentation of the tape data (Figure 14). By changing the gain and amplitude, and thresholding out certain upper and (or) lower limits, different levels of radiance can be enhanced. Quantizing and contouring of thermal infrared data are examples of this technique.

For example, the continuous curve of image density versus log of exposure (Figure 15) can be broken electronically into discrete steps of variable width-- all densities within each step being displayed in analog as a single density. Examples of density slicing of this sort are shown for thermal infrared data in Figure 16. The continuous-tone image is on the top, the n-level density-sliced equivalent in the middle. Electronic triggering at changes of density steps can produce a "spike" which can be displayed as a thermal contour, shown on the bottom on Figure 16. Ground temperature measurements or other control data can be used to convert this into a quantitative thermal contour map (the Michigan thermal scanner has internal calibrations, so that no ground control is required).

If each density slice is reproduced separately, copied on a colored transparent film and then the films stacked together, the result is a color-coded quantized thermal map (Figure 17).

Each of the 12 reflective and 5 thermal channels can be printed as video images comparable to that of Figure 14. These prints would constitute 17-channel multiband imagery. These images contain differences in tone (density)--hence, information--that is on or even below the limit of visual recognition, but that can be amplified or enhanced and made visible by electronic means. However, now that the data are recorded as signals on magnetic tape, they can easily be processed electronically in several ways to enhance selected features and to determine the statistical parameters of the spectral radiance (reflectance or emittance) of each class of material in the scene. This was done in analog form for data from the 12-channel scanner, that is, from the visible violet to the near infrared, or about 0.4 to 1.0 μm.

Specific targets in the scene can be selected. By electronically measuring the mean and standard deviation of the signals in each of the 12 channels, spectral signatures and covariance functions can be obtained for each target class, and the optimum channels for separating each object class from all other classes can be determined in the computer by spectral-matching or by maximum-likelihood statistical decision rules.

For example (Figure 18), radiance (a voltage now) is measured for each of the channels for water (W) and forest (F). A vertical line two standard deviations long, centered about the mean radiance, is shown for each of the 12 channels.

Note that these two classes overlap only in the reflective IR part of the spectrum (right side). Other materials overlap these two and each other in various places; some have dissimilar and others have closely similar spectral reflectance.

The radiance in channel 1 can be compared to that in channel 2 for each class of material. The distribution of this spectral covariance data might have the form shown diagrammatically in Figure 19, where each cluster represents a different material. R1 and R2 represent radiance in channels 1 and 2, respectively. A-D represent classes of material.

On a frequency diagram the covariance radiance data may appear like that shown in Figure 20, where the seemingly topographic surface is the surface that bounds the distribution of data points. R1 and R2 are radiance in channels 1 and 2, as before; f is the frequency of distribution of data.

This surface is topologically similar to, and can be considered as, a probability diagram. Each class (A-D) has its own peak value and falls off in all directions, generally in Gaussian fashion.

Statistically, if radiance values in channels 1 and 2 are r_1 and r_2, they fall under the peak of class A and should be classified as belonging to class A. They have high probability of belonging to that class. But values that fall in the regions of low relief are highly questionable in terms of which class they belong to. They have low probability values.

Part of the computer processing involves maximum-likelihood theory to establish what plane or contour level should be applied as a threshold limit--for instance outside the area of intersection of the "topographic" surface and the vertical cylinder (shaded) of Figure 20. Any value falling outside that area would be rejected for that class by the computer. For simplicity, the threshold limit (cylinder) is shown only for class A in Figure 20. The "contour" at which the thresholds are set for other classes may be different for each class, depending on the distribution of data (shape of the probability surface) and overlap of different classes.

The peak positions and the entire "topography" of this surface would be different in a plot of channel 1 vs 3, 1 vs 4 . . . 7 vs 9, 7 vs 10 . . . etc. The computer compares the radiance in channel 1 with that in 2, 1 vs 3, 1 vs 4 . . . 7 vs 9, 7 vs 10 . . . etc.--until all 144 combinations of the 12 channels have been computed. From this data, the complex 12 X 12 covariance matrix function is computed and stored for making decisions of classification. These data represent the multispectral characteristics or "signatures" of each designated terrain class. A diagram cannot be drawn to illustrate this 12-dimensional space--it exists only in a mathematical sense. That is why the computer is needed.

After the spectral distribution and the covariance functions are determined for all classes sought, the entire tape of the traverse can be run through and the computer instructed to recognize and show only areas whose spectral reflectance matches that of one class, for example FOREST. A photograph of the cathode-ray tube shows the distribution of all areas recognized as FOREST by this spectral matching technique (Figure 21).

Separate runs for recognition of other terrain classes can be printed in different colors and overlayed, resulting in a sandwich which is a colored map presentation of the data.

Although there are the advantages of real-time mapping of terrain units by having the analog computer in the aircraft during acquisition of data, for most scientific applications it has proven more feasible and more accurate to use digital programs to determine optimum channels and threshold levels and to feed this data back to the analog computer for the actual display and mapping in analog form.

DATA PROCESSING BY DIGITAL COMPUTER

Three basically different digital computer processing studies or tests were conducted. These involved:

1. Supervised programs using the scanner data
    a.   without preprocessing
    b.   with preprocessing of two different types

2. Non-supervised programs using the scanner data and clustering techniques

3. Non-supervised programs using the aerial color film and clustering techniques

SUPERVISED PROGRAMS

Although the digital and computer programs used at Purdue and at Michigan differ in detail, they are closely similar. The Purdue program was used without preprocessing of data; the Michigan programs were used to test different preprocessing techniques and to closely simulate the spectral response of the ERTS data channels.

TESTS WITHOUT PREPROCESSING

In contrast to processing the data in analog form such as that in Figure 14, they can be processed in digital form by making a digitized copy of the original magnetic tape. This is the procedure used by the Laboratory for Applications in Remote Sensing (LARS), Purdue University. This section of the report will discuss the Purdue method of handling multispectral scanner data, and preliminary results obtained on a section of one flight-line of the Yellowstone Park data.

This particular run was digitized in such a manner that, on the average, there was neither overlap nor underlap of adjacent scan lines (Figure 3). The scanner resolution is three milliradians, and the aircraft altitude was about 6,000 feet above terrain. This required that every 10th scan line be digitized. Also, each scan line contains 220 ground resolution cells. The scanner mirror rotates at constant angular rate whereas the digitizing was done at constant linear rate. This, plus the effect of topographic relief, changes the size and shape of the ground resolution cell from the midpoint to both ends of the scan line. Even so, the average dimensions of the ground resolution cell are approximately 20 by 20 feet. There is a gap of about 20 feet between cells along each scan line, making each cell effectively 20 by 40 feet.

The analog data were quantized to 8-bit accuracy. Therefore, each resolution element of each spectral band has one of 256 possible values.

A computer printout of the data from any given channel is made to simulate the analog video display by breaking the continuous tones of the gray scale into a finite number of discrete gray levels by assigning a letter or symbol to each level in accordance with the relative amount of ink each symbol imprints onto the paper. An example is given in Figure 22. Each of the 15 reflective and 2 thermal channels could be printed as video and (or) digital printout images, constituting 17-channel multiband imagery (for example, see Lowe, 1968, figs. 12a and 12b, p. 94 and 95). The area coordinates are fed to a computer system*, which then computes the statistical parameters of each class of material. These statistics are calculated from the relative response in each channel (Figures 23 and 24). Relative response can be considered as an uncalibrated reflectance measurement, where the lack of calibration between channels allows only relative comparisons of the various classes of materials within each channel. The statistical parameters calculated are based on an assumed Gaussian distribution of the data, and include the mean, standard deviation, covariance, and divergence (i.e., the statistical measure of the separability of classes). These statistics are stored by the computer, and are used to represent the multispectral characteristics of each designated class of material. These statistics constitute the

---

*An IBM 360 model 44 computer with 64K bytes (8 bits per byte) of core storage was used. The principal computer language used was FORTRAN, with ASSEMBLY used for some of the support programs.

multispectral pattern or "finger-print" of each terrain class, and are used in the computer program to 1) determine which channels are most useful for recognition of all object classes studied, and 2) actually classify the unknown data points into the known classes using a Gaussian maximum-likelihood decision scheme.

Four channels were used in the Purdue study. This decision was based on experience at LARS-Purdue which has shown that the use of only 4 of the 12 channels in the 0.4 to 1.0 μm range results in approximately as good a classification as does the use of more channels. Computer time, which increases in a geometric fashion with the number of channels used in the classification, is costly; therefore, some optimum for the number of channels used, the quality of results, and funds expended must be achieved. The channels selected are shown in Table II.

The channel-selection part of the computer program provides the capability of measuring the degree of separability of Gaussianly-distributed classes and determining the optimum set of channels for doing so. This is done by calculating the statistical distance in N-dimensional space between the classes, N being 12 in this case.

The classification part of the computer program involves the actual classification (mapping) of an arbitrary number of classes using an arbitrary number of channels and a Gaussian maximum-likelihood scheme. The display part of the program displays the results in line-printer form, and analyzes the recognition performance in each training area.

A thresholding capability is provided in the display process. If the resolution element does not exceed a predetermined threshold--that is, if the element does not look sufficiently like a member of the class to which it has tentatively been assigned even though that is the most likely class--then final classification of that element is declined and that element is assigned to a null class (rejected) and displayed as a blank. Different thresholds may be assigned to each of the classes individually.

A segment of the digital computer terrain map is shown in Figure 25. The part shown is composed of about 57,860 data points--about 22 percent of the full map. The full map covers an area of about 2 by 6 miles and is composed of 269,060 data points.

Initial processing disclosed that at least 13 classes could be separated. Several of these were subunits which have been combined to make the displays shown in Figure 25.

Hand-colored maps give a more graphical portrayal of the distribution of classes, but could not be reproduced here.

Table II. Channels used in the terrain classification and mapping, and to simulate the ERTS data channels using Purdue University's computer programs.

	Wavelength band used μm	Color or spectral region	Michigan scanner channel number
Best 4 channels	0.44-0.46	Blue-----------------------	2
	.62- .66	Orange----------------------	9
	.66- .72	Red-------------------------	10
	.80-1.0	Infrared--------------------	12
	.66- .72	Red-------------------------	10
	.80-1.0	Infrared--------------------	12
	2.0 -2.6	Infrared--------------------	--
	8.0 -14	Thermal infrared-----------	--
ERTS scanner channels:			
0.5-0.6 μm-----------	.52- .55	Green-----------------------	6
.6- .7 μm-----------	.62- .66	Orange----------------------	9
.7- .8 μm-----------	.72- .8	Infrared--------------------	11
.8-1.2 μm-----------	.8 -1.0	Infrared--------------------	12
ERTS RBV cameras:			
0.535 μm peak -----	.52- .55	Green-----------------------	6
.680 μm " -----	.66- .72	Red-------------------------	10
.760 μm " -----	.72- .8	Infrared--------------------	11

Thermal overlay

Another aspect of the work underway is a terrain classification made by substituting one or more data channels from the infrared scanners (1.0-14 μm) for those of the 12-channel scanner (0.4-1.0 μm).

For this test, channels 1, 3, 5, 7, 9, 10, 11, and 12 of the 12-channel scanner were combined with the 1.0-1.4 μm, 2.0-2.6 μm, 4.5-5.5 μm, and 8-14 μm channels. A computer program recently developed at LARS-Purdue made it possible to overlay the data from these two separate scanner systems. The computer selected the best set of four of these channels (Table II) for classification of the terrain in the same manner as before. The maximum mismatch of registry is no more than three ground resolution cells, and probably is mostly no more than one cell.

The "map" of Figure 26 is the result of overlaying one thermal and three reflective channels (0.66-0.72, 0.80-1.0, 2.0-2.6, and 8-14 μm). Only one of these channels is in the visible range. Because the scan angle of the thermal scanner was much narrower than that of the reflective scanner, this display covers only the middle east-west strips of those shown in Figure 25. The close correspondence of this display with the others indicates the accuracy of classification.

These studies should enable us to further extend the range of potential diagnostic spectra for existing classes and may point out some additional terrain classes. In addition, they will be useful tests of how well computer programs can take data from different scanner systems and automatically overlay them to produce a single set of multispectral data.

Simulation of ERTS data channels

Along with the studies of evaluating the accuracy of performance, we are studying how well data in wavelength bands tentatively designated for the proposed Earth Resources Technology Satellite (ERTS) might serve for automatic mapping of the same eight terrain classes in the same area.

The existing computer programs of Purdue did not allow a simulation of the wider wavelength band width of the ERTS sensors. Instead, the midpoints of the channels of the proposed ERTS 4-channel scanner, and the peak transmissions of the three Return Beam Vidicom (RBV) cameras were matched with the closest channels of the University of Michigan 12-channel scanner. These data are summarized in Table II.

The classification using the simulated ERTS 3-RBV cameras is shown in Figure 27. Note the close agreement with Figure 25--that based on the computer-selected best set of four channels. A segment of the display of the simulated ERTS 4-channel scanner data classification is shown in Figure 28, for comparison with the RBV camera simulation and the computer-selected 4-channel display (Figures 25 and 27).

Accuracy

In general, the products are highly satisfactory terrain maps which portray PHYSIOGRAPHIC UNITS or units which are unique associations of ROCK-SOIL-VEGETATION

The following generalizations about accuracy of classification of the terrain classes is based on comparison of the computer-generated maps with the ground control data.

1. BEDROCK EXPOSURES
    This class is present mainly in the western part of the test area, along the banks of the Yellowstone River, and in a quarry where it was moderately well classified. Where misidentified, it generally was classified as vegetated rock rubble--a closely similar unit into which it grades.

2. TALUS
    All of the known areas of this class and a few previously undetected are clearly delineated.

3. VEGETATED ROCK RUBBLE
    The general areas classified are realistic, but in detail this class is the least well classified. Because of the small size of the individual areas occupied by this unit, it is not possible to locate precisely a homogeneous training area.

4. GLACIAL KAME MEADOW
    Areas of kame meadows are accurately depicted. Areas of forested kame sand
    and gravel between open meadows of kame were erratically classified by the
    computer, mostly as other units. Control data show that in some places this
    class occurs as small scattered patches surrounded by till; in those places
    it was misidentified by the computer.

5. GLACIAL TILL MEADOW
    This class was first classified as four separate subunits on the basis of
    change in illumination across the flight path, but the four were later
    combined into one unit for the map printout. Classification is estimated
    as about 95 percent accurate over the entire flight strip. The other
    classification symbols scattered throughout areas of this class generally
    are correct, for there are small areas of vegetated rubble and of bogs in
    meadow areas underlain by till.

    Although both the till and kame deposits are the sites of meadows, the
    differences in amount of soil exposed and the subtle differences in soil
    composition and texture apparently permit these two classes to be accurate-
    ly distinguished by the computer.

6. FOREST
    This class generally is well recognized in large, almost uniformly-symboled
    blocks. All forest areas seem to be consistently recognized. Local
    clusters of deciduous trees were recognized separately, but combined with
    evergreens in the displays.

7. BOG
    This is one of the best recognized classes. All known bogs and many pre-
    viously unknown small bogs were correctly mapped.

8. WATER
    The Yellowstone River and Floating Island Lake (see Figure 5) were clearly
    recognized. Phantom Lake (not on this segment of map) was dry at the time
    of flight, and so was correctly classified as bog rather than water. Parts
    of the Yellowstone River were omitted or generalized, principally because
    the width of the river is near the threshold of resolution, and because
    some data points were integrated values of river plus some other class or
    classes. Stretches of white-water rapids were rejected. In places, the
    shaded north edges of patches of forest were printed as scattered points
    of water or talus.

9. SHADOWS
    All shadows were recognized well.

10. OTHER
    All data points whose reflectance did not closely fit the statistical data
    for any of the above nine classes were rejected, and shown as blank regions
    on the map. A few of these are very light and bright areas of shallow
    water where bottom deposits show through, or are white-water rapids and
    gravel bars.

A blacktop road can be detected in places as a line of anomalous symbols, but is not consistently recognized as any particular class. The road is about as wide as a single data point and hence is at the threshold of resolution.

Although all bedrock types were classified as a single unit, the spectral reflectance histograms, spectrograms, and the divergence data indicate good possibility of distinguishing among several of the rock types present. Further testing over areas of larger rock exposure seems justified.

Where terrain classes covered large areas, they were correctly identified by the computer. Most inaccuracies occurred where the units were small and where some were below the threshold of resolution; accordingly, the radiance for a given resolution cell was a complex combination of several classes. Presumably, the computer usually selected the dominant terrain class or, by thresholding, indicated that the spectral properties did not clearly fit any of the classes.

For comparison of the performance of classification using the ERTS simulations with the best sets of four channels, the computer rated itself in the training areas only. For example, of the total of 5,418 data points used in training the computer, less than 20 of those were subsequently classified (using the best set of four channels) as something other than what they were called during the training. The ratings are as follows:

Best set of four channels------------------------------99.6 percent
Thermal overlay--------------------------------------98.8
ERTS 4-channel scanner-------------------------------97.7
ERTS 3 RBV---93.8

The figures are a good measure of the <u>relative</u> accuracy of each test. They are misleading in part because the computer assumes that each training area is homogeneous, consisting 100 percent of what it was labeled. The 0.4 percent error probably is a close measure of the degree of inhomogeneity of the material in the training areas.

When coordinates of other known areas (test areas) are fed to the computer, the computer determines the classification of those areas and computes the accuracy of classification. Appraisal of numerous test areas gives a more complete and meaningful evaluation of the overall recognition performance of the computer program.

Preliminary results of computer studies which rate the accuracy of classification of test areas give the following overall performance (data from unpublished report by Marc G. Tanguay):

Best set of four channels------------------------86 percent
Simulated ERTS four channels---------------------83
Simulated ERTS 3-RBV cameras---------------------82
Thermal overlay----------------------------------81

These figures should be taken as approximations only. They agree with a preliminary visual estimate that the overall accuracy of all displays is more than 80 percent, and indicate that the best set of four channels gives slightly better results than the other three displays, all of which are about equally good.

The drop in accuracy from 99 to 86 percent, etc., from the training to the test areas, is understandable, because we would expect the computer to perform well in the areas where it was trained unless the reflectances of two or more classes were closely similar in all channels used.

For the training areas, the classification made using the overlay of thermal and reflective channels was virtually as accurate as the best classification-- that using the computer-selected best set of four reflective channels (98.8 vs 99.6 percent, respectively). However, for the test areas, the thermal overlay was least accurate (about 81 vs 86 percent). The slight mismatch of registry in parts of the thermal overlay test undoubtedly results in a less accurate classification than if all channels were in complete registry, as would occur if a single scanner system could cover the range of 0.4 to 14μm or more.

Nevertheless, these studies indicate that the infrared region is promising in the classification of some terrain units. For example, in the test areas the thermal overlay classification was better than the computer-selected best four-channel classification for glacial till (95 vs 93 percent), glacial kame (82 vs 74 percent), and bog (81 vs 80 percent). The accuracy of classification of talus in the test areas was only about 49 percent; however, most of the error was due to talus being misclassified as vegetated rock rubble, a unit which actually is quite similar to talus. If talus and rock rubble are combined as a single unit, the accuracy jumps to about 83 percent, whereas the same combination was classified only about 76 percent when using the best set of four channels in the test areas.

In geologic applications it is more desirable to know what kind of material the forest is growing on than simply to know where the forest is. The thermal overlay classification has some potential in this regard; it has been shown (Waldrop, 1969) that thermal infrared in forested areas can in places indicate the sites of thick, unconsolidated, well-drained gravels vs bare or thinly man- tled bedrock.

An obvious advantage of infrared data channels for space applications is the haze penetration ability. Further investigations are needed to adequately assess the potential of these channels, particularly over areas of extensive rock outcrops.

Studies underway also include careful evaluation of the overall accuracy by point-to-point comparison with ground-truth maps. It is important to recall the recognition of previously undetected areas of occurrence of some terrain units. This means that errors in the control maps are being detected at the same time errors in the computer printout are being sought.

In general, the ERTS simulations differed from the computer-selected best four channels as follows:

1.   For areas correctly shown as FOREST on the classification using the best four channels, the ERTS 4-channel classification showed small to moderate amounts of TALUS and WATER, whereas the RBV 3-channel classification showed greater amounts.

2.   In places, both ERTS classifications showed considerably more BOGS than are present in areas that were correctly classified by the best four channels.

3.   Slightly poorer classification of water was performed in the ERTS classification.   However, few of the bodies of areas of water in the test area are of sufficient size to serve as good training areas, so I do not view this part of the classification as a good test of the ability of the ERTS data channels to permit automatic identification of water.

I wish to point out that these are not complete simulations of the ERTS data channels, but are only first approximations, because no attempt was made to simulate 1) the poorer resolution of the satellite sensors due to vast differences in scale, 2) the effects of atmospheric attenuation, or 3) the broader wavelength bands of most of the ERTS sensors (see Table II). Studies at the University of Michigan aimed at more closely simulating the actual wavelength bands of the ERTS sensors, are described in a later section of this report.

All four of the experiments produced good results. They are good classifications. I do not wish to set any specific limits on how good "good" is. Obviously, some are better than others, and none is perfect--but neither is the man-made control map--and preprocessing of the data, as described below, further improves the accuracy of the computer-generated maps. I am convinced, however, that all can be considered as more than adequate for the reconnaissance first-approximation kind of interpreting and mapping which we expect to accomplish with the satellite data.

TESTS OF PREPROCESSING OF DATA

Programs for terrain classification using multispectral data, such as described above, are based on the assumption that the spectral radiance of all objects of a given class in the scene is substantially the same. During these studies we soon determined that this was not true because of various factors such as cloud shadows, haze, variations in topography, and changes in scanner "look" angle. As a result, the performance of classification schemes based on spectral signatures was degraded, both in analog and digital tests. This was partly overcome by selecting multiple training sets for each class, each set effective over a narrow range of data along the scan line. However, this lengthened the preparation and computer-processing time. This is described more fully in a paper by Smedes, Spencer, and Thomson (1971).

Preprocessing of the data to compensate for the angular variations was studied using digital computer programs developed by the University of Michigan. This allowed the use of a single training set for each class of objects anywhere in the field of view. It shortened the preparation and computer-processing time, gave more accurate results, and, in places, enabled areas under cloud shadow to be classified as to the correct terrain class.

In a way shadows and topography pose similar problems, in that they affect the total level of irradiance. North-facing slopes, and shadows, result in lowering the total level, whereas south-facing slopes reflect more light back to the sensor and result in a raising of the total level. However, in both cases, the ratio of observed (recorded) spectral radiance in two spectral channels will be independent of variations in the level of radiance.

The topographic and other scan-angle-dependent variations may be deduced and corrected for by dividing by a function of the scan angle.

Results of preprocessing cf these two types--ratio transformation and scan-angle function transformation--are described below.

Ratio Transformations

Three ratio preprocessing techniques, previously reported by Kriegler and others (1969), make use of the fact that if the scene radiance varies, this variation is present in all spectral channels. Ratios of channel signals therefore will show less variation with scene changes than will the signals themselves.

These ratio transformations, which have been previously used as techniques for preprocessing the scanner-spectrometer data to reduce illumination variations, are:

1. Ratio of each channel to the sum of all channels, e.g., $\dfrac{\text{channel 1}}{\Sigma \text{channels}}$.

2. Ratio of adjacent channels, e.g., $\dfrac{\text{channel 2}}{\text{channel 1}}$.

3. Ratio of the difference to the sum of adjacent channels, e.g., $\dfrac{\text{channel 2 - channel 1}}{\text{channel 2 + channel 1}}$.

If the original scanner-spectrometer data consist of N channels, then after performing any of these three ratio transformations there would be (N - 1) independent channels of data. Therefore, one channel must be eliminated. Arbitrarily, the twelfth channel was eliminated in these studies by Michigan. The data of Table III show that the first ratio transformation (ratio of each to the sum) gives lower probability of misclassification than do the other two ratio transformations.

Table III. Probabilities of misclassification of training area classes using different preprocessing of the original data and ERTS scanner simulations. The higher the value, the greater the probability of misclassification.

Preprocessing technique	Probability of misclassification		
	Best channel	2 Best channels	3 Best channels
Ratio transformation 1 $\left(\dfrac{\text{channel } n}{\Sigma \text{ channels}}\right)$	0.088 (n=1)	0.037 (n=1,5)	0.026 (n=1,5,10)
Original data ERTS RBV simulation ERTS scanner simulation	0.101	0.039	0.035
Ratio transformation 2 $\left(\text{channel } \dfrac{12}{11} \text{ etc.}\right)$	0.179 $\left(\dfrac{12}{11}\right)$	0.087 $\left(\dfrac{12}{11}\right), \left(\dfrac{10}{9}\right)$	
Ratio transformation 3 $\left(\dfrac{\text{channel } 12 - 11}{\text{channel } 12 + 11} \text{ etc.}\right)$	0.186 $\left(\dfrac{12 - 11}{12 + 11}\right)$	0.091 $\left(\dfrac{12 - 11}{12 + 11}\right), \left(\dfrac{10 - 9}{10 + 9}\right)$	
Normalized scan-angle function transformation	0.070 (5)	0.015 (5, 12)	0.009 (5,12,2)

Scan-angle Transformation

More knowledge of the scene is required for the use of this preprocessing technique than for the ratio preprocessing. It is assumed that the variations in scene radiance in each spectral channel can be described by a function of scan angle, which may be determined by analyzing spectral signatures from one or more classes of materials distributed along the scan line. Enough information must be available to locate samples of a given class of material at various scan angles.

If the ratio of spectral radiances of two classes as a function of scan angle is constant, then we can derive a single correcting function which we can assume will be valid for all data in each spectral channel for all classes. This assumption is equivalent to assuming that the bidirectional reflectance variations as a function of scan angle of different classes are the same.

A universal scan-angle correcting function for each channel is obtained by normalizing the function of signal vs scan angle for any one material at some particular scan angle.

For one spectral channel (channel 1, Table I), the variation in the means and standard deviations of the training areas of FOREST, BOG, and TILL as the scan angle is varied are shown in Figure 29. In this example, a radiance value of 0.8 could be interpreted as any. one of the three classes depending on the scan angle.

Figure 30 shows the same data after the scan-angle transformation. Now the classes are clearly separated, and a radiance value of 0.8 could only be interpreted as TILL.

If the preprocessing technique is successful, the wide separation in mean values of spectral signatures of classes at different scan angles (Figure 29) has been eliminated for training sets of the same class of material. One could easily obtain combined signatures for each class using unpreprocessed data, as was done in the Purdue study. Because this results in signatures with large standard deviations, the signatures of different materials are far more likely to overlap, causing increased probabilities of misclassification. Because of this, the Purdue tests using non-preprocessed data required that most materials be treated as subunits, in terms of scan-angle position--the subunits later combined as complete units (classes) during the printout stage.

As with the non-preprocessed data studied by Purdue, the Michigan computer program* utilizes a supervised training program which involves a maximum-likelihood decision scheme for selecting the best spectrometer channels, and closely similar techniques of digitizing the data of the analog magnetic tapes.

Studies of the training areas of all classes enabled the computer to calculate the probability of misclassification by using the different preprocessing techniques described above. The results, summarized in Table III, indicate that use of the normalized scan-angle function transformation would result in the lowest probability of misclassification. Hence, that transformation was used in making the recognition map of Figure 31. The symbols used to designate the different terrain classes are shown in Table IV.

Simulation of ERTS Data Channels

The existing Michigan computer programs allowed a closer simulation of the full band width and spectral response of the ERTS sensors.

---

* A CDC-1604 computer with 32K bytes (8 bits per byte) of core storage was used. The computer language used was FORTRAN IV. An IBM-1401 computer was used for peripheral work and for the actual printing of the recognition of maps in color.

Table IV. <u>Symbols and colors used to represent the different terrain classes</u>
<u>shown on the maps of Figures 28, 31, and 32.</u>

Material	Color				
	Blue	Red	Green	Black	White
Bog			*		
Forest			ℳ		
Glacial Till Meadow		ℳ			
Glacial Kame Meadow		*			
Bedrock	ℳ				
Vegetated Rock Rubble	*				
Water				ℳ	
Talus				*	
Shadow				.	
Not classified					(No Symbol)

    The spectral responses* of the ERTS 4-channel scanner and the three RBV
cameras were used to construct nominal spectral sensitivity curves. The detailed
spectral response of each scanner-spectrometer channel (Larsen and Hasell, 1968)
were fitted graphically to the specified ERTS data using a technique described by
Nalepka (1970). Further corrections to account for peak sensitivity variations
in photomultipliers were determined from radiance standard lamp data. The result
was a set of weighting coefficients to be assigned to each spectrometer channel
to simulate the ERTS sensor data. These are summarized in Table V.

    These data were used with the signatures previously obtained from the train-
ing areas, using preprocessing with the ratio transformation in which the spectral
channel is divided by the sum of spectral channels, using channels 1, 5, and 10
(see Tables I and IV). The terrain map made using this data is shown in Figure
32.

---

* Data obtained by F. Thomson and M. Spencer of the University of Michigan
from L. Goldberg and O. Weinstein of NASA-Goddard.

Table V. Weighting factors for simulation of ERTS sensors with original scanner spectrometer data.

Michigan spectrometer channel number	ERTS 4-channel scanner and RBV camera	Weighting of Michigan channels
5		0.68
6	channel 1	.86
7		.98
8		.70
8		.74
9	channel 2	.96
10		.72
11	channel 3	1.00
12	channel 4	1.00
4		.72
5	camera 1	.82
6		.95
7		.86
9	camera 2	.94
10		.59
11	camera 3	1.00

The probability of misclassification of training area classes using simulated ERTS scanner data is 0.035 (Table III) and the average percentage of correct recognition is 81 (Table VI). Although no recognition map was run for the simulated ERTS 3 RBV cameras, the data from the training areas indicate probability of misclassification as 0.039 using the same ratio transformation. If the simulations had been made with normalized scan-angle transformation, the probability of misclassification surely would have decreased, and the accuracy of recognition would probably have increased to about 90 percent (deduced from data of Table VI).

Accuracy

The accuracy of classification using preprocessing techniques of the original spectrometer data and the simulated ERTS scanner data is indicated in part by the data of Table VI, which is based only on the training areas.

The ERTS simulations were made using the best of the three previously tested ratio processing techniques before Margaret Spencer had developed and tested her program for normalized scan-angle preprocessing. Had the scan-angle preprocessing

been used, it would have permitted use of all four ERTS channels rather than the three which resulted from the (N - 1) loss inherent in all ratio preprocessing techniques, as described above.

Table VI. <u>Accuracy of recognition in training areas using different preprocessing of original spectrometer data and ERTS scanner simulations (maps of Figures 28, 31, and 32)</u>.

Catagory	Results of training area evaluation of the recognition map, in percent correct recognition		
	Normalized scan-angle transformation	Ratio transformation $\left(\dfrac{\text{channel n}}{\Sigma \text{ channels}}\right)$	ERTS scanner simulation using $\left(\dfrac{\text{channel n'}}{\Sigma \text{ channels}}\right)*$
Bedrock	96.7	80.0	47.7
Talus	91.9	81.0	63.1
Vegetated Rock Rubble	94.4	91.9	95.3
Glacial Kame Meadow	100	93.3	94.7
Glacial Till Meadow	98.6	74.4	89.0
Forest	97.0	88.8	85.5
Bog	95.0	92.7	88.9
Water	94.7	94.7	93.4
Shadows	97.4	91.8	71.3
Average percentage of correct recognition	96.2	87.7	81.0
Average percentage of incorrect recognition	3.4	11.6	18.4
Average percentage of no recognition	0.4	0.7	0.6

* n' indicates the simulated ERTS channel which is a non-linearly weighted summation of several original spectrometer channels (see Table V) and does not correspond to n which represents the non-weighted original spectrometer channel.

The simulated ERTS data gave poor results for three classes--bedrock, talus, and shadows. However, bedrock and talus basically are exposures of rock blocks, the blocks in talus simply having moved down slope a short distance, and the two units actually are gradational. If these two gradational classes are combined, the recognition performance would rise to values comparable to those of other classes, for nearly 18 percent of the bedrock was misidentified as talus and nearly 28 percent of the talus was misidentified as bedrock. The apparently poor performance of the ERTS data for shadows (71.3 percent) is misleading because

10.4 percent of the training area was identified as forest, which is the true terrain unit that was under the shadow. This suggests that, somehow, the simulated ERTS data can "see" through the shadow better than can the other recognition techniques.

As with the non-preprocessed data, the most meaningful test of accuracy is not in the areas for which the computer was trained, but throughout the entire map, through use of numerous test areas or a point by point comparison with the ground control data.

At the time of this writing, studies are underway to determine more closely the accuracy of these preprocessed classification maps. Preliminary results indicate that the most important improvement in accuracy has resulted from the fact that, because of preprocessing, the area of shadow was markedly reduced and the true terrain unit beneath the shadow accurately mapped. Because the terrain class generally under cloud shadow was forest, the classification of forest was greatly improved over that of the non-preprocessed maps.

In comparing the accuracy of these maps made using preprocessing techniques with those made without preprocessing, the following generalizations are valid: bog, glacial kame meadow, water, and vegetated rock rubble were as accurate or slightly more accurate; forest, glacial till meadow, bedrock, and talus were definitely more accurate.

Thus, in spite of far fewer training areas (24 vs 187) and fewer channels used (3 vs 4), these maps are more accurate and required less computer time than those made without preprocessing.

NON-SUPERVISED PROGRAMS

The various techniques described above required that we train the computer on known areas. This requires some prior knowledge of the region. The techniques described below are based on non-supervised processing that requires no prior knowledge of the area. These techniques utilize the fact that the radiance of different classes tends to cluster in different places in n-dimensional space. The programs allow the computer to determine these clusters and to plot each class based on clustering, whatever the class may be.

One such natural class might be printed in map form by the letter S, for example; and, although you would not know what that class really was, you would know everywhere it occurred. Limited field checking or photo interpretation would then give an identity to each of the classes mapped by this clustering technique.

In addition to the fact that no prior knowledge is required, there is the further advantage that no calibration is required.

Non-supervised digital computer processing of data using cluster techniques has been done using the multispectral scanner data and color aerial film.

SCANNER DATA

In order to reduce computer time, the original twelve channels of data were preprocessed by a principal-components analysis to yield four different classes, but with almost all (more than 99 percent) of the statistical and spatial structure preserved. The cell size was reduced by taking every third row of resolution cells and every third resolution cell on each such row taken. This is the equivalent of a cell 60 by 60 feet. Each of the four classes consists of a binary vector of 25 components.

From this principal-components analysis, clustering and inverse clustering functions (described briefly below) were generated for a sample of 1,908 data elements out of 30,044.

Any clustering procedure assigns data elements to clusters such that the elements within a cluster are closely similar or related, and elements of any two clusters are dissimilar or unassociated.

The clustering technique used at the University of Kansas is an iterative clustering procedure (Haralick and Dinstein, 1970) programmed for the GE 635 computer.

Viewed as a geometric approach, the data elements are represented as vectors of N binary components, each of which has a value of +1 or -1. Hence, each data element can be considered as a vertex of an N-dimensional unit hypercube in an N-dimensional Euclidian space. The clustering function f projects those points into vertices of a K-dimensional unit hypercube. The points that are projected into a vertex of the K-dimensional hypercube form a cluster whose code is the coordinates of the vertex in the K-dimensional space. The inverse clustering function g projects these vertices of the K-dimensional hypercube back into some vertices of the N-dimensional hypercube.

The computer program enables the K-dimensional hypercube to be iteratively "rotated" until the sum of the distances between the original and respective projected-back data points is minimum.

The f and g functions are chosen from a class of parametric functions derived from linear threshold functions. "Rotation" of the K-dimensional hypercube is accomplished by iterative small changes in these parameters.

The cluster map derived from this iterative clustering technique by digital computer contained symbols delimiting four classes. These classes were outlined, traced onto a blank sheet and coded with drafting patterns. This final product is shown in Figure 33. The classes correspond generally with the following:

        Black = Rock
        Dark gray = Till on south-facing slopes (low elevation) and
                    local patches of mixed vegetated rock rubble, forest,
                    and rock on south-facing slopes (low elevations)

Medium gray = Till, kame, locally vegetated rock rubble
White = Forest, water, and shadow

The topographic and scan-angle functions have obviously degraded the class-ification as indicated by the different patterns for materials along the north edge (south-facing slopes at low elevation). Preprocessing by ratio or scan-angle function transformations undoubtedly would improve the accuracy.

COLOR AERIAL FILM

Traditionally, multispectral data from film have been from multilens cameras using black and white film, each lens filtered to pass only a limited wavelength band. In the present study, conducted with EG&G, Inc., the three emulsion layers of color infrared film were used as a three-band spectrometer. This film was ac-quired at the same time as was the scanner data. Because of the focal length of the cameras, the film covers only the central part of the full scan width.

This study is underway at the time of this writing, so only preliminary results can be presented in this report.

The three emulsions of color infrared film are most sensitive to the broad spectral bands (approximate) listed below, as normally exposed with appropriate filters:

Emulsion	Color recorded	Band width	Equivalent spectrometer channel numbers
blue	green	0.50-0.58μm	5,6,7
green	red	.58- .68	8,9,(and half of 10)
red	infrared	.68- .90	10,11,(and half of 12)

Image density data from each of the three color emulsions were entered into a digital computer program that produces terrain maps by using clustering techniques.

The 70-mm color transparencies were scanned by a Mann Trichromatic Micro-densitometer at a resolution of 450μ, corresponding to a spot about 30 feet in diameter on the ground. All three color film layers were sampled simultaneously by means of beam-splitters and filters. Triads of density values were obtained from each area element on the transparency, as shown diagrammatically in Figure 34, and were recorded on magnetic tape. The data were digitized to nine-bit accuracy (though less accuracy would suffice). Characteristic spectral signa-tures inherent in the data--presumably representing terrain classes--were iden-tified by the application of clustering techniques in three-color space. Each datum point was assigned on the basis of its spectral signature, to one of these classes, and each class was then assigned a letter character (for example, A and B, Figure 34). Computer-generated overlays were made to fit photographic en-largements of the transparency at a scale of approximately 1:4,000 (Figure 35). Existing control data enabled these classes to be labeled as to true terrain class. This technique is described more fully in a paper by Smedes, Linnerud, and Hawks (1971).

The following terrain classes were automatically mapped from color infra-red film, with overall accuracy equal to or better than those of previous multi-spectral scanner classification (better than 85 percent): 1) deciduous trees, bushes, and bogs, 2) evergreen trees, 3) bedrock, largely granitic gneiss, and rhyolite tuff (in a quarry), 4) bedrock, largely basalt and amphibolite, 5) talus, 6) rock and talus in shade, and 7) shade of trees and cliffs.

The resolution cell size of the present study closely simulates the computer-generated maps previously made from multispectral scanner data. Studies underway include classification of the same areas using smaller ground area elements.

The present study indicates that color film can be used as an accurate means of multispectral terrain mapping by computer. An important additional advantage is that the results can be directly overlaid on the photograph. Geometric dis-tortions can be rectified by using stereoscopic pairs of aerial photographs and simple standard photogrammetric techniques. Color aerial photographs are readily available at low cost, whereas scanner data are sparse and are expensive to obtain.

The widths of the bands used in this study are similar to those of the ERTS sensors. The accuracy of classification (better than 85 percent) indicates how well the ERTS sensors might be expected to perform in classifying similar terrain, and agrees closely with the results of ERTS simulations made using scanner data.

CONCLUSIONS AND RECOMMENDATIONS

Direct comparisons cannot be made between any of the computer maps and the control data for several reasons. With the exception of the test with the color aerial photos, it is not possible to transfer the class boundaries accurately from the scanner format to the topographic base map or to annotated aerial photos on which the control data are plotted. Scanner distortions and size of the com-puter ground resolution cell place constraints on the accuracy of locating these boundaries. Continuing research and development at the Universities of Michigan, Kansas, and Purdue are minimizing these constraints.

The control data consist of a surficial geologic map, a bedrock geologic map (both of which ignore the vegetation), and a map in which percentage of classes within broader areas are indicated (Figure 36). Thus, because we cannot accurate-ly locate and check accuracy of mapping of specific small clumps of trees or small and scattered outcrops, we can only compare percentages of these classes within the broader areas on the computer map with those on the generalized control map. But, for the purposes of these tests, we are really only interested in the larger features, anyway--those that constitute a large resolution cell comparable to that which can be resolved by the satellite sensors.

Furthermore, a direct comparison cannot be made of the results obtained using different computer techniques because of the differences in digitizing the data, number and size of training areas used, and resulting differences as sum-marized below. However, the objectives of the Michigan study were principally to test the effectiveness of preprocessing and of more closely simulating the ERTS data channels.

	Purdue	Michigan
Total number data points	269,060	187,131
Number of training areas	187	24
Total number of data points in training area	5,418	3,521
Percent of total area used for training	2%	1.9%
Maximum number of channels used in classification	4	3

The University of Kansas cluster processing used only every third row of cells and every third cell of such a row, resulting in a ground resolution cell of about 60 X 60 feet in contrast to the cells of 20 X 20 feet and 30 X 30 feet used in the other tests. However, in this regard, it more closely simulates the resolution of the satellite sensors.

In spite of this inability to be able to make a point by point (cell by cell) comparison of the computer maps with the control data, the overall accuracies can be rather well determined, as indicated in previous chapters.

One of the overwhelming problems of automatic mapping of terrain classes is that the spectral signatures of a given class vary widely with such things as time of day, season of the year, latitude and flight direction (illumination-angle functions), and recency of rain in the region. I doubt that we can adequately sample the spectra of many classes of material under a wide enough range of conditions so that by the spectra alone we could identify materials.

Lacking complete samples of spectral signatures, we would have to rely on supervised computer techniques, thus requiring some prior knowledge of the terrain.

However, after studying the results of these tests, and on the basis of discussions with Dr. Robert Haralick of the University of Kansas, I am convinced that there is great potential in the cluster processing technique, and that automatic mapping will be most successful where the two kinds of processing--non-supervised and supervised--are performed in concert. Specifically, I suggest that the (non-supervised) cluster techniques be used to determine what the natural terrain classes are and where they are. Then, sample spectra of these classes can be compared to spectral signatures in a master computer data bank to determine which class or classes of material most closely correspond to the spectra from these natural terrain classes. Although several specific classes may be equally likely on the basis of the data bank, several may be eliminated by mutual exclusiveness with adjoining classes, by reference to model studies such as described by Watson at this Workshop, or by some very general knowledge of the region surveyed. It may thus be possible to identify specific natural classes of terrain without field check.

Preprocessing of the data is an important part of the concept because it normalizes the data and thus minimizes the effects of variations in illumination due to scanner "look" angle, topography, and shadows. Subsequent sets of data over the same area could be processed using conventional supervised techniques.

If we examine the spectral range spanned for each of the displays (Tables II, V, and Figure 37), we see that they vary by a factor of nearly 50, from 0.28 μm for the 3-camera ERTS system to 13.34 μm for the thermal overlay classification. This implies that, for a broad range of terrain categories, many combinations of three or four channels of data in the 0.4-14 μm range would be satisfactory. More complete simulations, in which the effects of the atmosphere are considered, undoubtedly will require identification as to which channels would be suitable. For example, the haze penetration ability of some reflective infrared channels, mentioned earlier, is an obvious advantage for satellite applications; the blue part of the spectrum is apt to have low signal-to-noise ratio and therefore be of limited use except for oceanography. We need worry about careful selection of specific wavelength bands only if a specific category is being sought. Inasmuch as the ERTS program is aimed at covering many scientific disciplines and user groups--hence involving many terrain categories--the highly specific requirements are not now pertinent to tests of the suitability of the proposed satellite sensors.

I believe that the concept, rather than the specific immediate results of these studies, is the most important product. Admittedly, it is not really important to find that talus occurs on the shore of a lake here or that a narrow bog lies there--we already know most of that for this particular area. The important point is that eight or more widely different terrain units could be accurately mapped automatically. For the moment it does not really matter what the units are or where they occur--they could as easily have been orchards, barns, municipal parks surrounded by streets and buildings, beaches, polluted or clean water, marshlands, etc.

In fact, I believe that these particular maps are over-classified in comparison with what we will want to attempt from space--at least for our first attempts. It may well suffice to map out such features as WATER, VEGETATION, BARE SOIL, and ROCKS, and to interpret other things, such as geologic structure, from the resulting patterns and their relations to topography.

Especially significant applications in geology and other fields will be for those features that are time-dependent, changing with the seasons or with a few years' time. Once an area has been mapped by computer, the areas of change can be periodically mapped automatically in terms of material, location, and the amount of area changed

I suggest that economically feasible geologic applications will include those that contribute to regional mapping, engineering geology, hydrology, and volcanology. Other applications may be in the fields of agriculture, cartography, land-use and land-management studies, and in still other fields in which seasonal and other changes are more rapid than in most geologic applications. In many fields, these data will become more useful by combining them with other (nonspectral) data--for example, the engineering application to trafficability studies--by combining these terrain data with slope (from radar images or topographic maps).

The fact that we are sensing surface material emphasizes the need for multidisciplinary approach to terrain mapping, because the surface involves the complex interplay of at least bedrock and surficial geology, hydrology, soils, vegetation, and meteorology. Traditionally, in mapping many regions of the earth, we interpret the geology secondarily from the patterns of other materials and features.

I hope that, in this brief review of the steps involved in acquiring and processing the data, you can see in the results some applications to your own fields of interest.

ACKNOWLEDGMENTS

REFERENCES

More detailed information on optical-mechanical scanners and the various techniques and computer programs described in this report can be found in the following. Those cited in this report are preceded by an asterisk.

Cardillo, G. P., and Landgrebe, D. A., 1966, On pattern recognition: Purdue Univ. Laboratory for Agricultural Remote Sensing Inf. Note 010866, 18 p. mimeographed.

*Haralick, R. M., and Dinstein, I., 1971 (in press), An iterative clustering procedure, in Institute of Electrical and Electronics Engineers Trans. Systems Science and Cybernetics.

*Kriegler, F. J., Malila, W. A., Nelapka, R. F., and Richardson, W., 1969, Preprocessing transformations and their effects on multispectral recognition,

in Proceedings of the Sixth Int. Symposium on Remote Sensing of Environment.: Ann Arbor, Michigan Univ. Inst. of Science and Technology, v. 1, p. 97-131.

Landgrebe, D. A., and staff, 1968, LARSYAA, A processing system for airborne earth resources data: Purdue Univ. Laboratory for Agricultural Remote Sensing Inf. Note 091968, 34 p. memeographed.

*Lowe, D. S., 1968, Line scan devices and why use them, in Proceedings of the Fifth Symposium on Remote Sensing of Environment: Ann Arbor, Michigan Univ. Inst. of Science and Technology, p. 77-100.

*Smedes, H. W., Linnerud, H. J., and Hawks, S. G., 1971, Digital computer mapping of terrain by clustering techniques using color film as a three-band sensor, in summary of papers presented, Seventh Int. Symposium on Remote Sensing of Environment, May 17-21, 1971: Ann Arbor, Michigan, Univ. Mich.

*Smedes, H. W., Pierce, K. L., Tanguay, M. G., and Hoffer, R. M., 1970, Digital computer terrain mapping from multispectral data, and evaluation of proposed Earth Resources Technology Satellite (ERTS) data channels, Yellowstone National Park: Preliminary report: Am. Inst. of Aeronautics Earth Resources Observations and Information System Mtg., Annapolis, Md., March 1970; AIAA Paper No. 70-309, 18 p.

*Smedes, H. S., Pierce, K. L., Tanguay, M. G., and Hoffer, R. M., 1970, Digital computer terrain mapping from multispectral data: Journ. of Spacecraft and Rockets, v. 7, no. 9, p. 1025-1031. (This is a condensed version of the AIAA paper listed above.)

*Smedes, H. W., Spencer, M. M., and Thomson, F. J., 1971, Preprocessing of multispectral data and simulations of ERTS data channels to make computer terrain maps of a Yellowstone National Park test site, in summary of papers presented, Seventh Int. Symposium on Remote Sensing of Environment, May 17-21, 1971: Univ. of Michigan, Ann Arbor, Michigan.

Swain, P. H., and Germann, D. A., 1968, On the application of man-machine computing systems to problems in remote-sensing: Purdue Univ. Laboratory for Agricultural Remote Sensing Inf. Note 051368, 10 p. mimeographed.

*Waldrop, H. S., 1969, Detection of thick surficial deposits on 8-14 infrared imagery of the Madison Plateau, Yellowstone National Park: U.S. Geol. Surv. open-file report, 7 p., 2 figs.

Watson, Kenneth, 1971, Geophysical aspects of remote sensing, in Proceedings of the Int. Workshop on Earth Resources Survey Systems.

Willow Run Laboratories Staff, 1968, Investigations of spectrum-matching techniques for remote sensing in agriculture; final report, January 1968 through

September 1968:   Ann Arbor, Michigan Univ. Inst. of Science and Technology
Infared and Optical Sensor Laboratory report no. 1674-10-F, 48 p.   This
report contains numerous pertinent references.

GLOSSARY OF SPECIAL TERMS USED

Basalt lava. Fine-grained, dark colored lavas relatively rich in calcium, iron, and magnesium, and low in silica.

Breccia (volcanic). A rock formed of compacted volcanic fragments embedded in a tuff matrix.

Cathode ray tube. A vacuum tube that generates a focused beam of electrons which can be deflected by electric and/or magnetic fields. The terminus of the beam is visible as a spot or line of luminescence caused by its impinging on a sensitized screen at one end of the tube. These tubes are used to re-produce pictures in television receivers or to study the shapes of electric waves.

Control data. This refers to all that is known about the site conditions, in-cluding types and distribution of materials (determined from conventional field mapping and examination supplemented by study of photographs taken from the air and ground), and measurements of such parameters as tempera-ture, relative humidity, porosity, moisture content, and spectral reflec-tance of surface materials. Collectively, these constitute the control data with which the test data can be compared.

Covariance. The manner in which one feature or parameter varies in relation to another.

ERTS. Acronym for the Earth Resources Technology Satellite.

Gneiss. A coarse-grained metamorphic rock in which bands rich in granular min-erals alternate with bands in which platy minerals predominate. These are derived from pre-existing impure sandstone, shale, or granite during the dynamic and thermal processes involved in mountain-building.

Kame. A mound composed chiefly of gravel and sand, whose form is the result of original deposition by settling during the melting of glacier ice against or upon which the sediment accumulated.

Maximum-likelihood. The maximum probability or chance. The statistical para-meters of radiance may somewhat resemble those of two (or more) different classes of material. The relative likelihood (probability or "odds") that the data in question belong to class A as opposed to class B or C is $P(A)/P(B)$ or $P(A)/P(C)$. When the statistical parameters are chosen so that these ratios are optimum, then the likelihood is maximum and the data are assigned to that class (A,B, or C) which has maximum probability.

μ **m**. Micrometer; the millionth part of a meter. Formerly called micron.

Rhyolite. Fine-grained, light colored lavas and other igneous rock bodies relatively rich in potassium, sodium, and silica, and low in calcium, magnesium, and iron.

Solifluction. The process of slow downhill flowage of masses of soil and uncon-
solidated surface debris saturated with water.

Till. Nonsorted, nonstratified sediment carried or deposited by a glacier.

Tuff. A rock formed of compacted volcanic ash and other fragments generally
smaller than 4 mm in diameter.
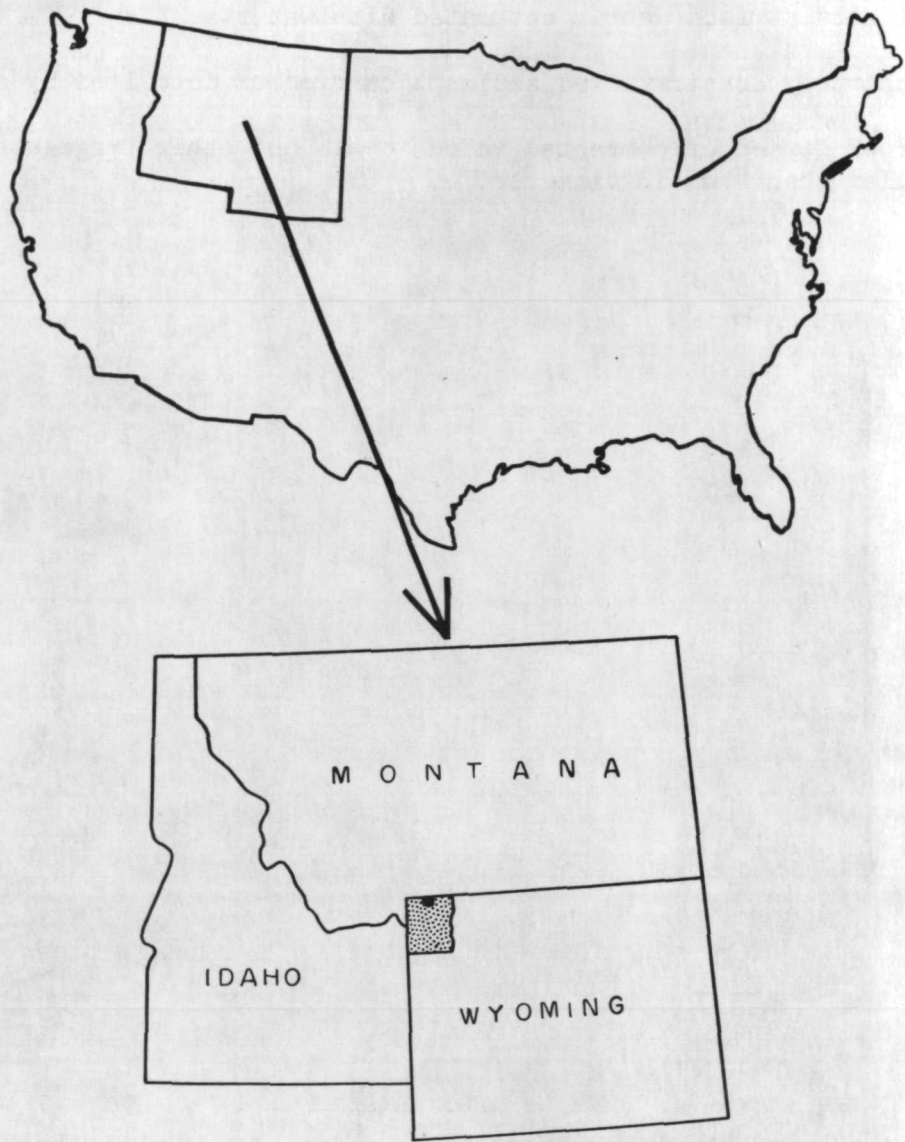
Figure 1. Index map of United States showing location of Yellowstone
National Park (shaded) and the test site (black).

Figure 2.   Panorama photo of test site looking west from near east edge.   Crescent Hill is on the left edge.
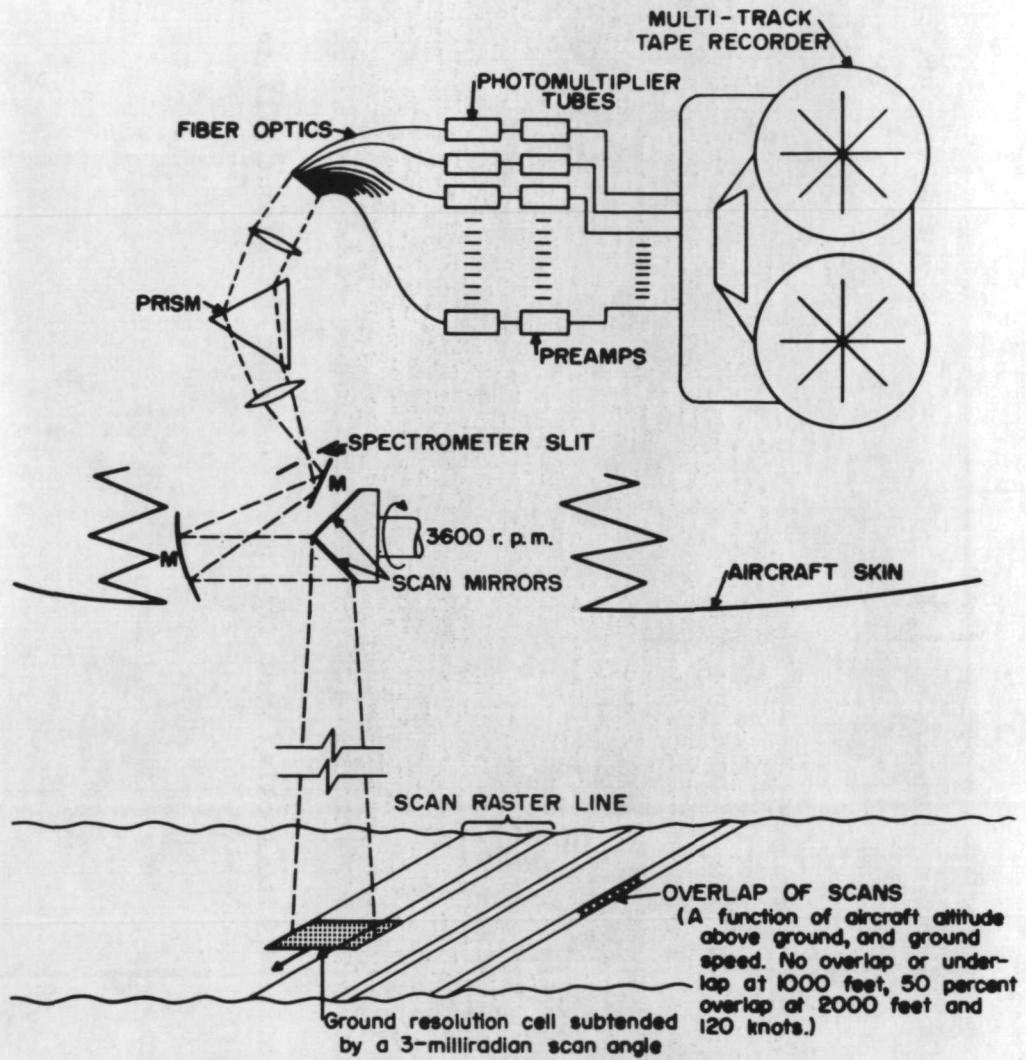
Figure 3.   Diagram of optical-mechanical scanner and spectrometer used by the University of Michigan in gathering data for this study.

Figure 4. Bedrock exposure of basalt lava flows.
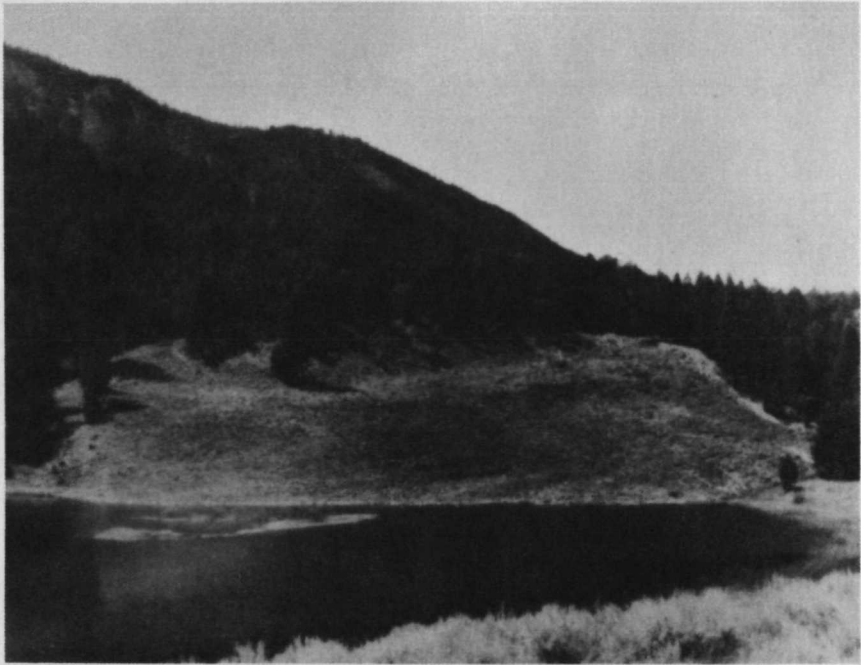
Figure 5. Talus of rhyolite tuff at Floating Island Lake. Crescent Hill is in the background.

Figure 6. Blocks of rhyolite tuff in talus showing contrast between fresh surfaces (below hammer head) and surfaces coated with dark lichens, which is what the scanner records.

Figures 7 and 8. Vegetated rock rubble. These are mixtures of angular
  blocks of basalt (fig. 7), bedrock slabs and blocks of gneiss (fig. 8),
  lichens, soil, dry grass, sagebrush, weeds, evergreen seedlings, and
  twigs.

Figure 9

Figure 10

Figures 9 and 10. Glacial kame meadow, showing grass, mineral soil, weeds, dead vegetation, elk manure (fig. 9) and sagebrush debris (fig. 10).

Figures 11, 12, and 13. Glacial till,
showing sand, rock chips, and boulders
in mineral soil, grass, sagebrush, weeds,
and twigs. Wide range in texture is
shown: fine-grained (fig. 11), mixed
(fig. 12), and coarse-grained (fig. 13).
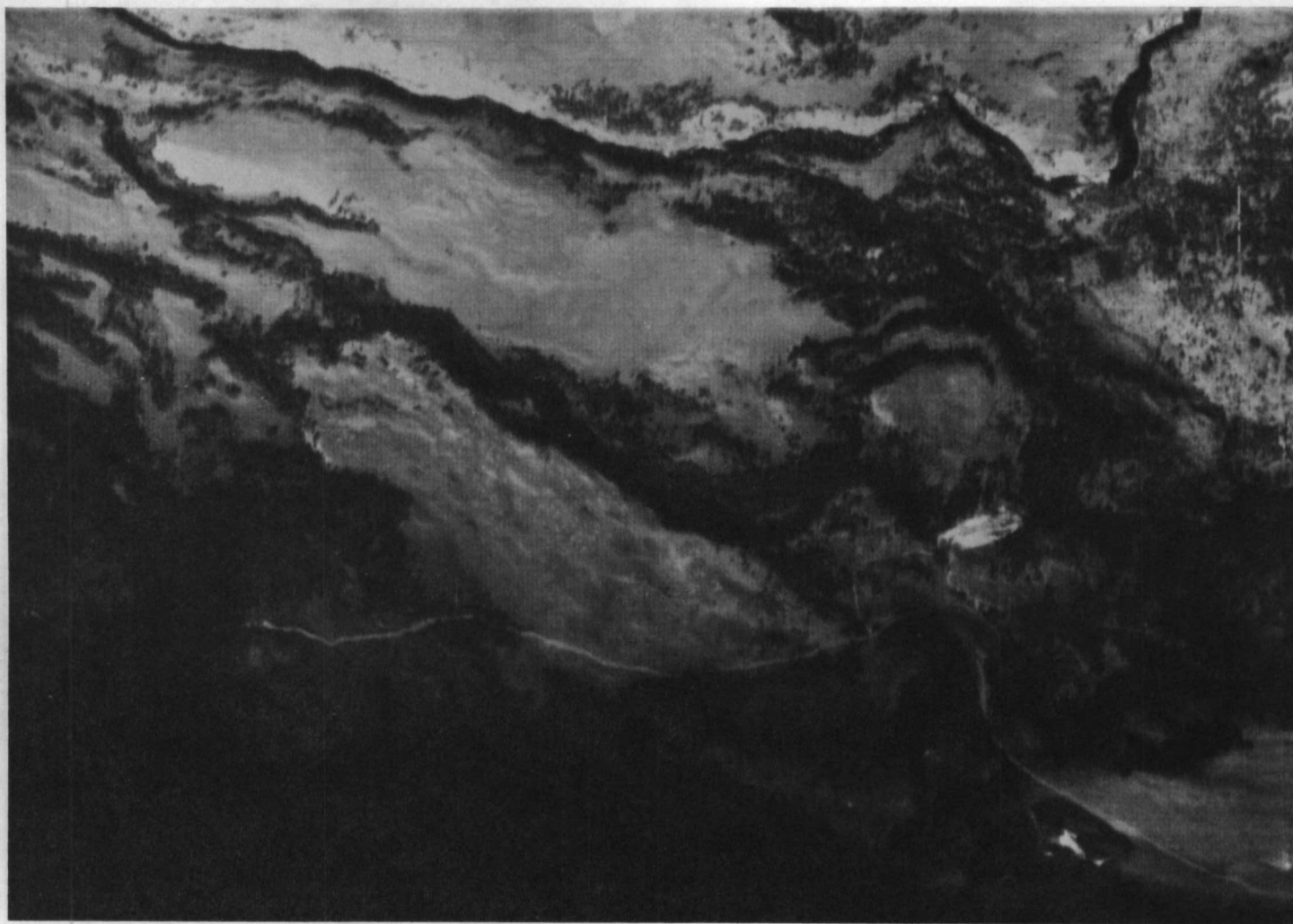
Figure 14. Gray-scale video display of radiance from channel 9 (0.62-.66 μ m). Area is same as shown in eastern parts of figures 26 thru 30.
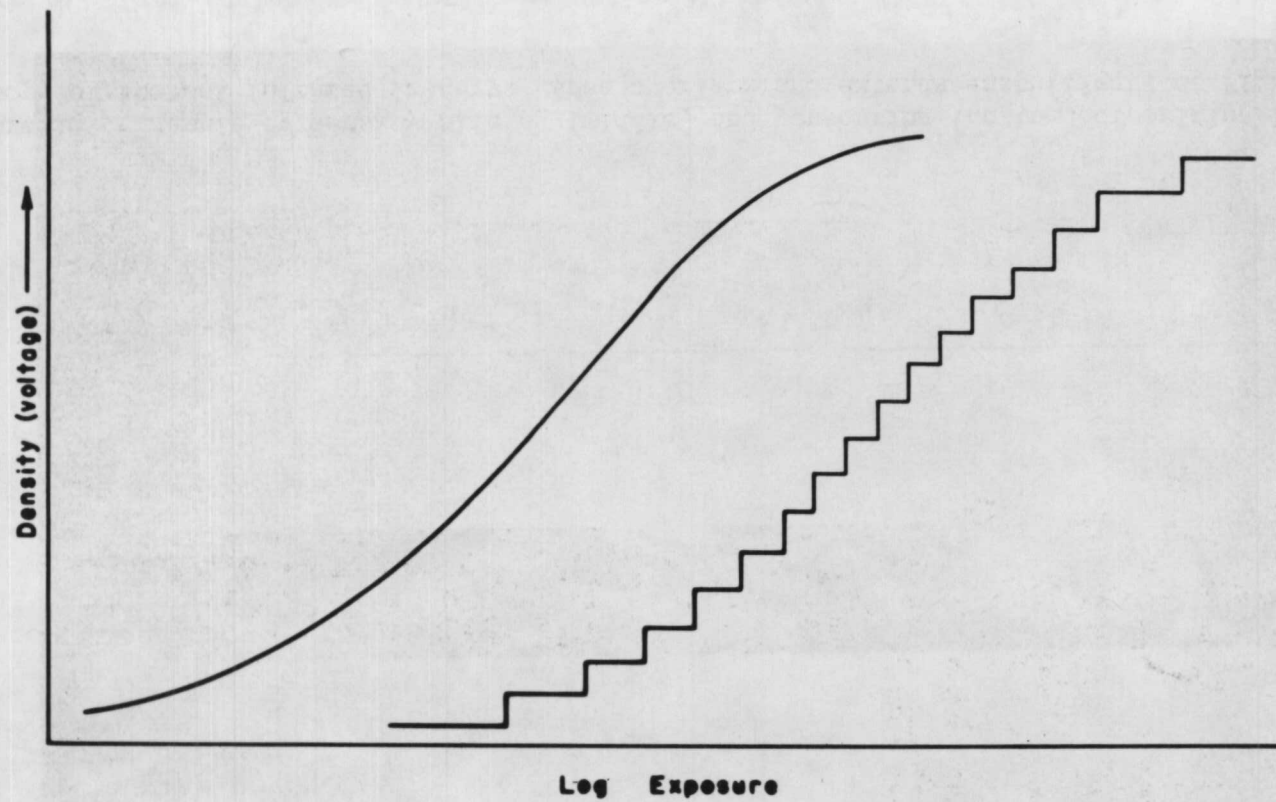
Figure 15. Example of electronic density slicing of continuous curve of film density (on the left) into discrete steps (on the right).
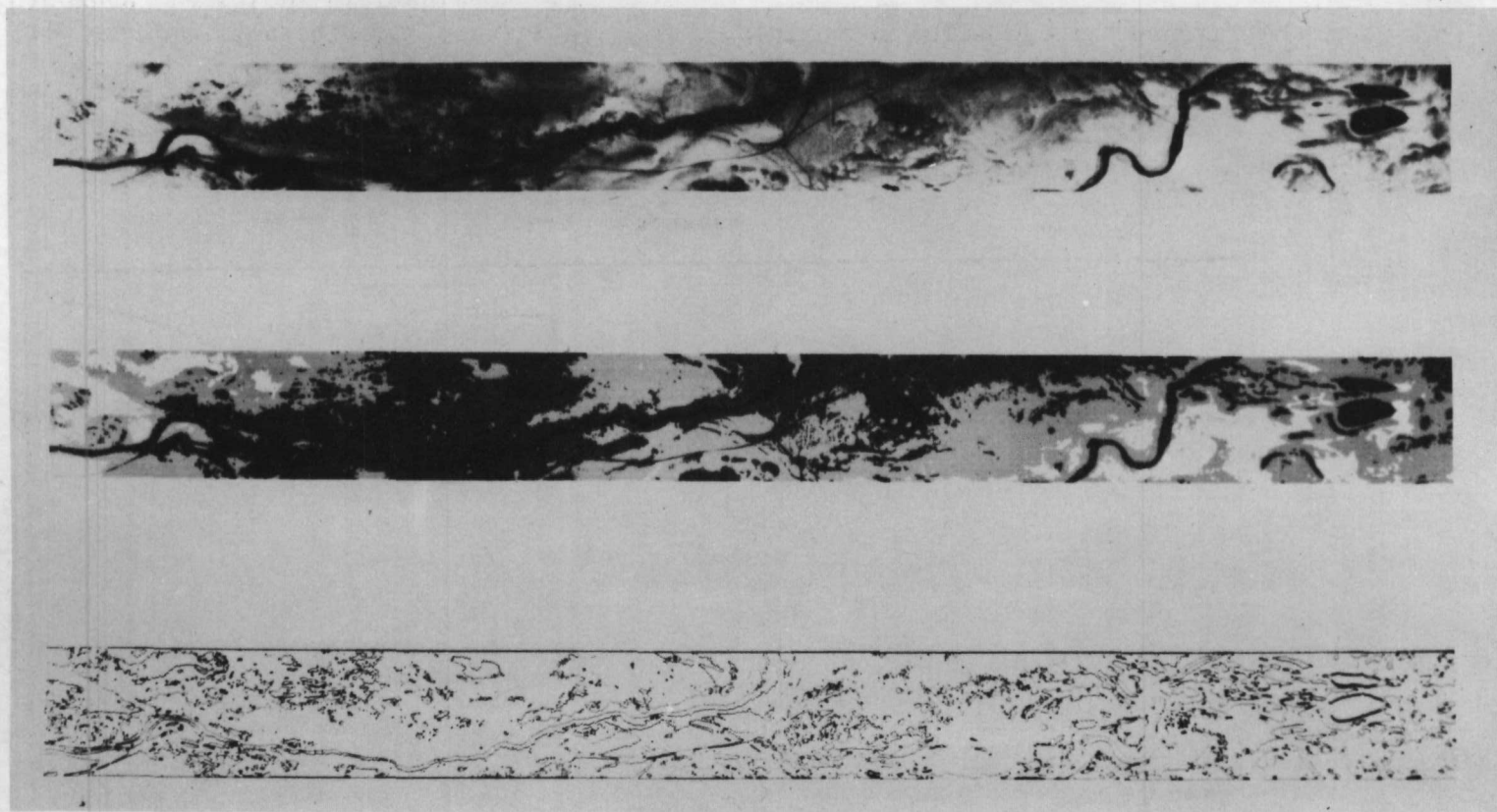
Figure 16. Example of density slicing (middle) and contouring (bottom) of originally continuous tones (top) of thermal infrared imagery. Area overlaps and extends east (right) of Figure 14.
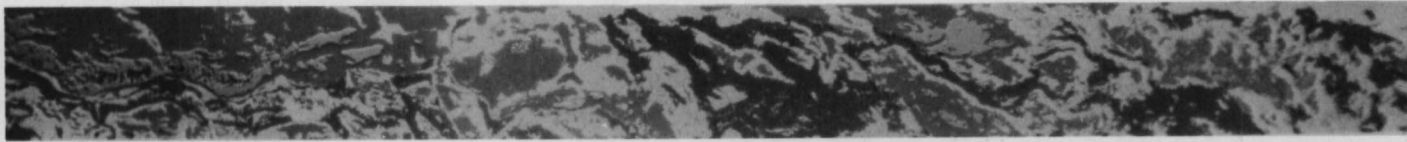
Figure 17. Color coded quantized thermal infrared image. Temperatures, from coldest to warmest, are shown on original color print by white, blue, yellow, red, green, and black, but are portrayed by different shades of gray on this black and white copy.
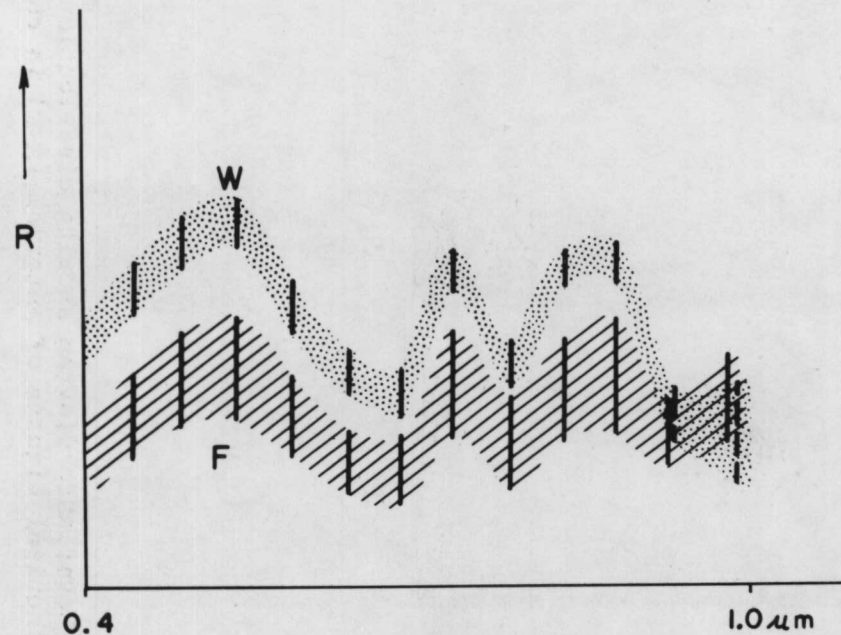
Figure 18. Radiance of water (W) and forest (F). Radiance (R) increases upward. A vertical line two standard deviations long, centered about the mean radiance, is shown for each of the 12 spectrometer channels.
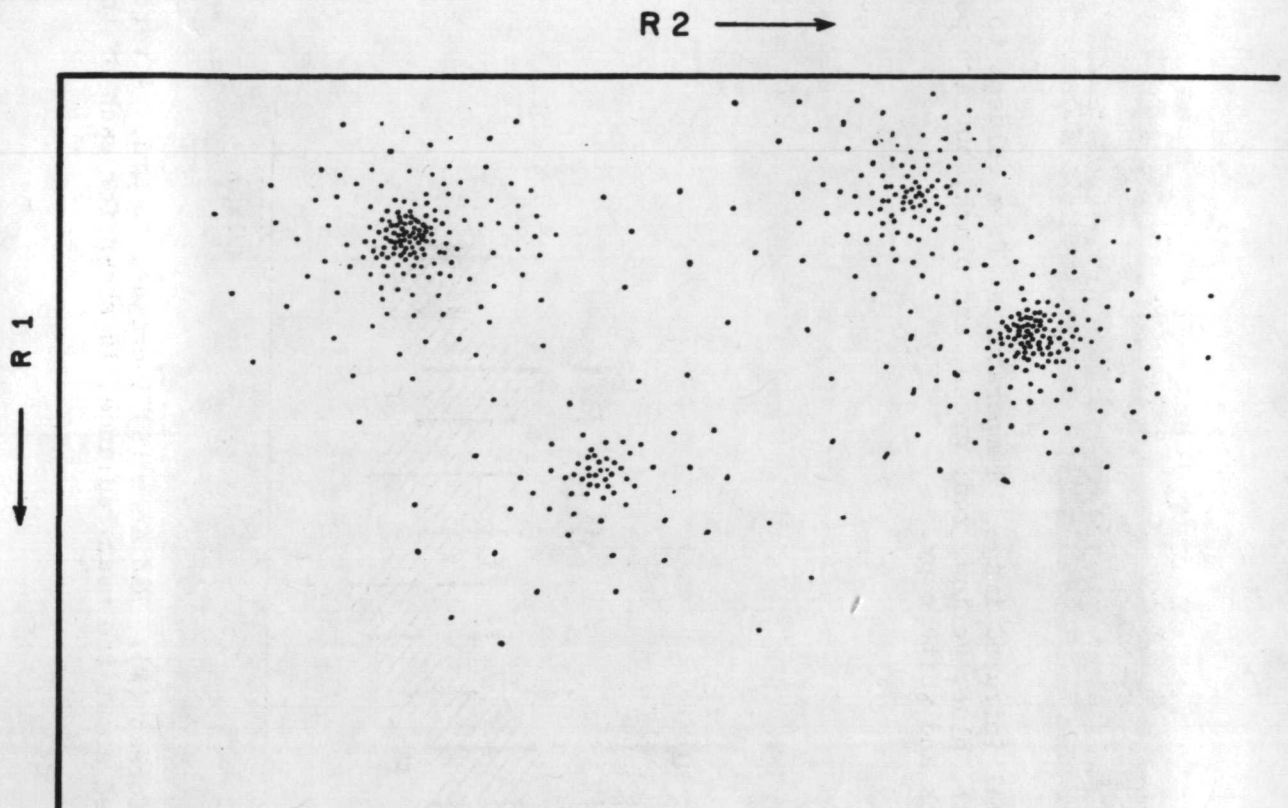
Figure 19.   Covariance diagram showing distribution of radiance data for
four hypothetical classes of material (A-D) in channels 1 and 2
(R1, R2).
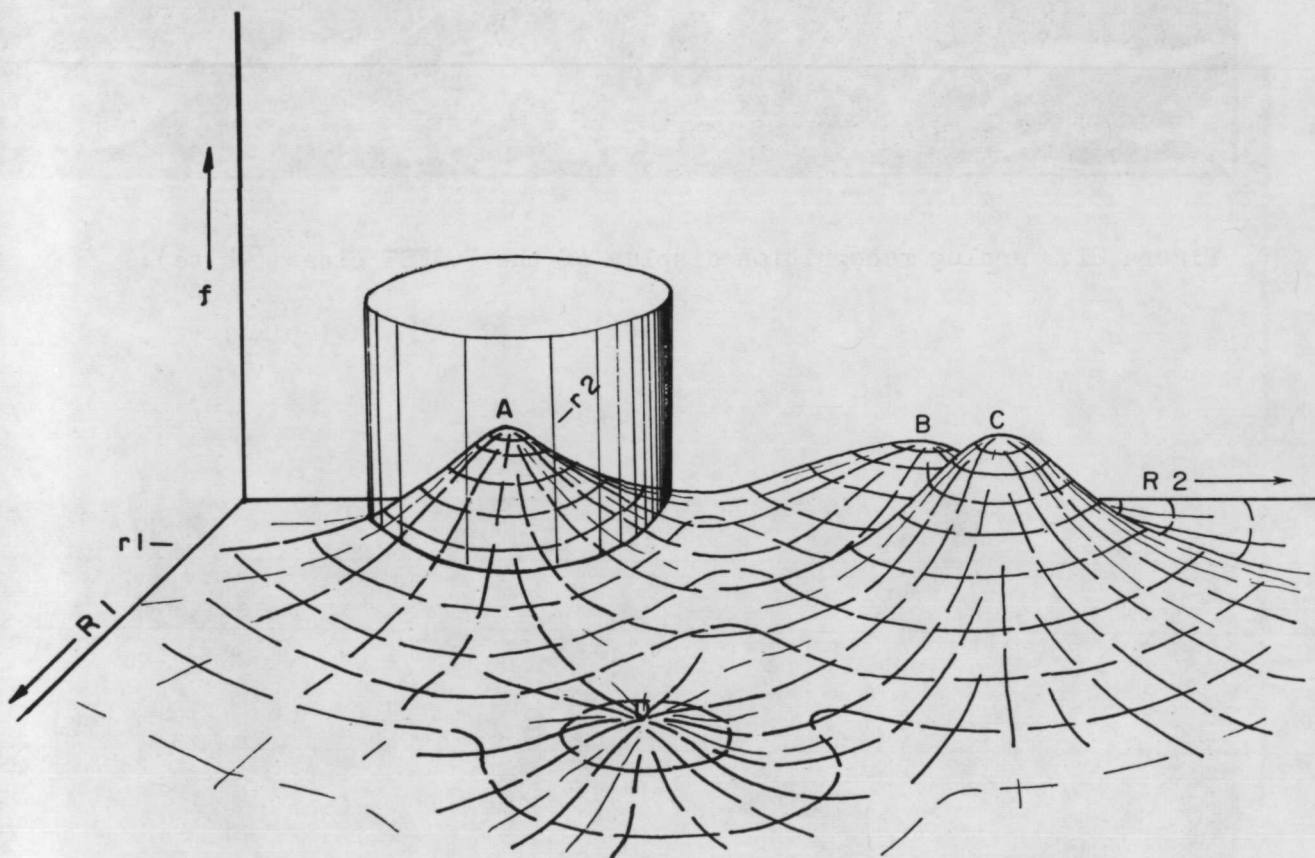
Figure 20. Frequency diagram of covariance data of same four classes (A-D) and channels (R1, R2) as in figure 19. The surface is that which bounds the distribution of data points, and is topologically equivalent to a probability surface. The cylinder indicates placement of threshold limits; for simplicity, it is shown for class A only.
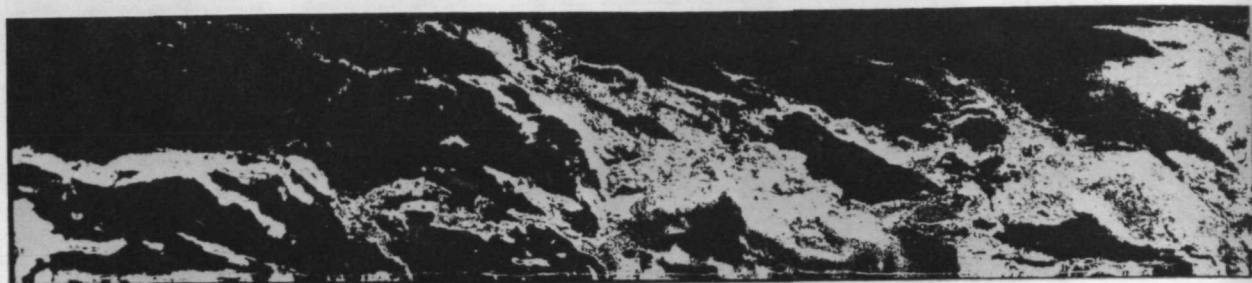
Figure 21. Analog recognition display of the FOREST class (white).

Figure 22. Ten-level gray-scale digital computer display of radiance from channel 9 (0.62-.66μ m), as obtained by University of Purdue. Area shown is the bottom (south) half of that shown in Figure 14.
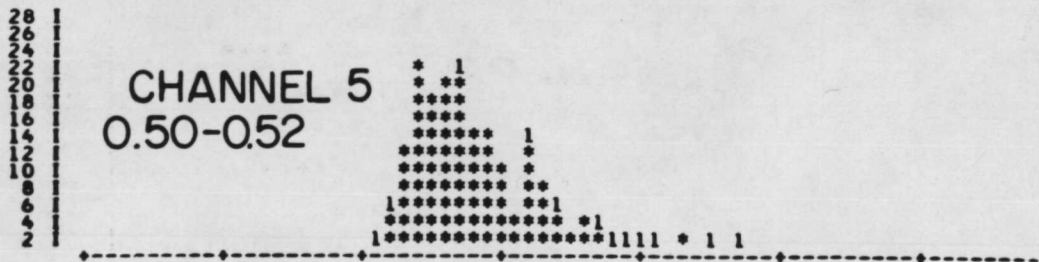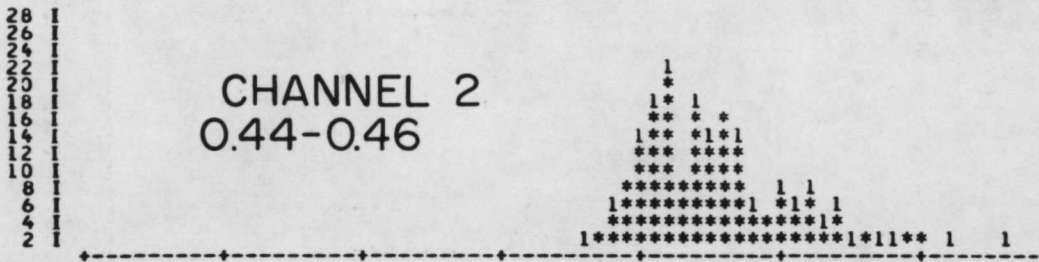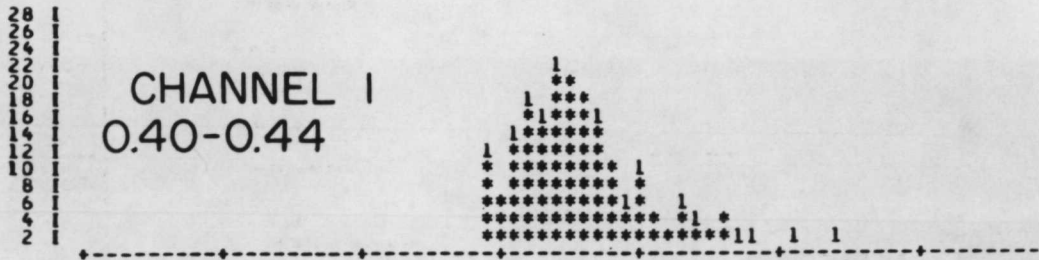
Figure 23. Histograms of reflectance of talus in channels 1, 2, and 5. The abscissa is relative radiance (brightness), increasing to the right. On this copy of the computer printout, the ordinate gives the number of resolution elements with a given relative radiance. Band width of each channel given in micrometers.

OFF SCALE   (+) 62   (+) 31

SPECTRAL BAND (MICRONS)

0.40 0.44	0.44 0.46	0.46 0.48	0.48 0.50	0.50 0.52	0.52 0.55	0.55 0.58	0.58 0.62	0.62 0.66	0.66 0.72	0.72 0.80	0.80 1.00
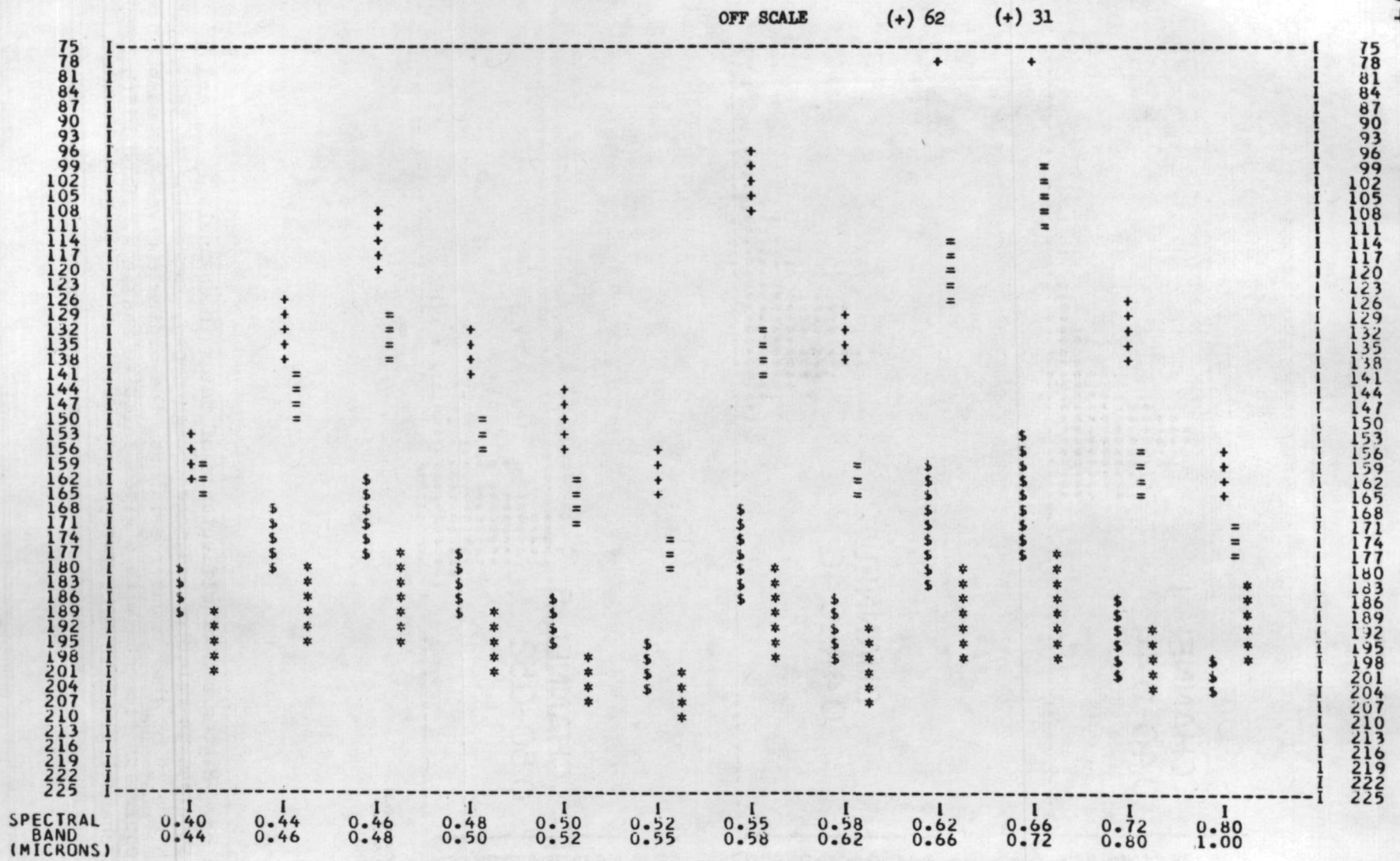
Figure 24. Comparisons of spectral reflectance of training areas of four classes of material: $ Talus, + Vegetated rock rubble, = Kame, * Forest. Reflectance or radiance, increasing upward, is shown for each of the 12 channels of the Michigan scanner data. A vertical line two standard deviations long, centered about the mean radiance, is drawn using alphanumeric symbols.
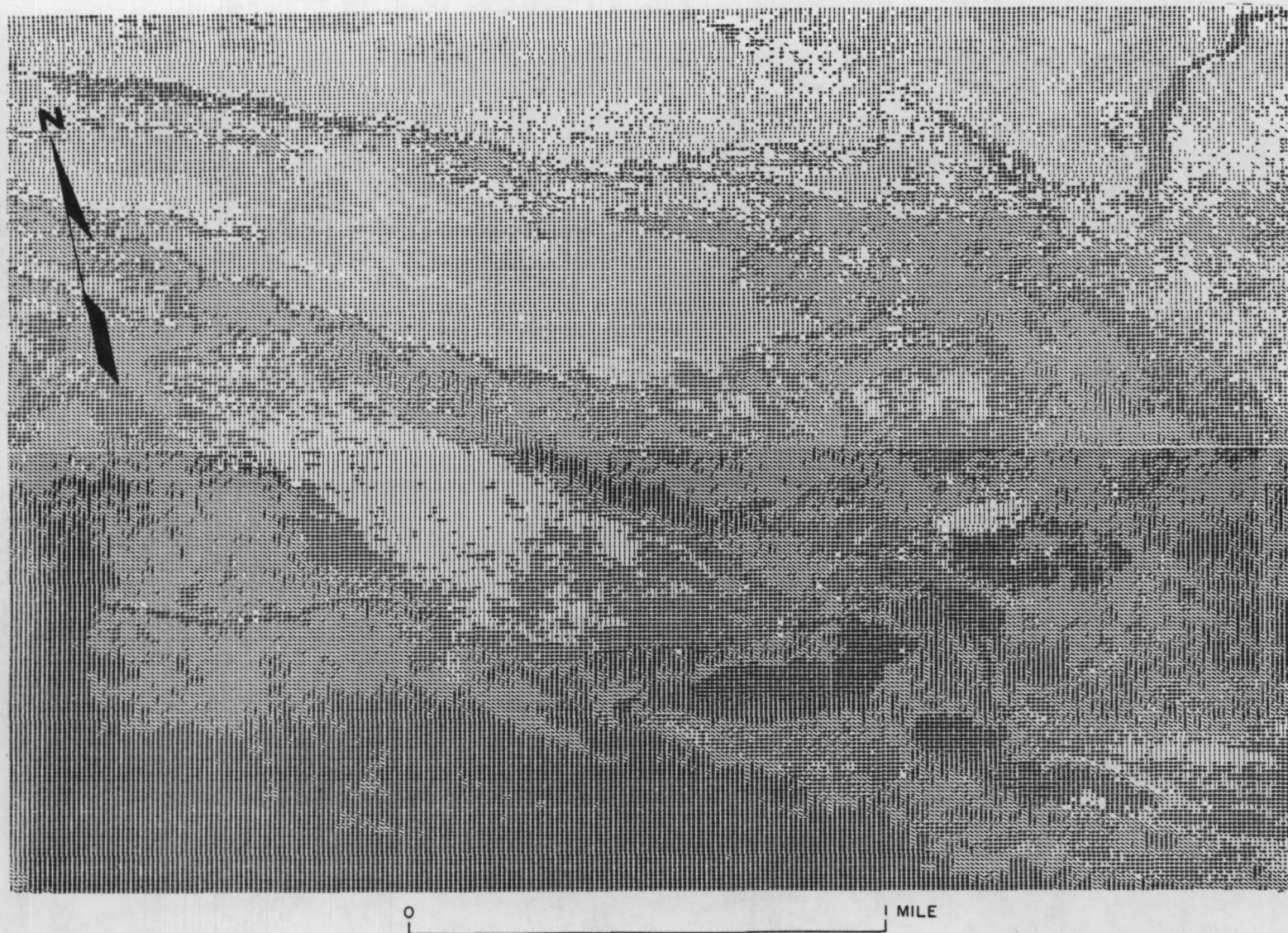
Figure 25. Segment of terrain map obtained by using Purdue University's digital computer-selected best set of four channels of radiance data. Symbols used to designate the terrain classes are:
. Bedrock Exposures, $ Vegetated rock rubble, - Glacial till meadows, : Bog, H Shadows, 8 Talus, = Glacial kame meadows, / Forest, W Surface water, (Blank) Rejected.

396

Figure 26. Segment of terrain map obtained by combining one thermal infrared and three reflective
channels of data. Symbols used to designate the terrain classes are the same as in figure 25
(water and bedrock are not present in this display). Because the scan angle of the thermal
scanner was much narrower than that of the reflective scanner; this display covers only the
middle strip of those shown in figures 25, 27, and 28.
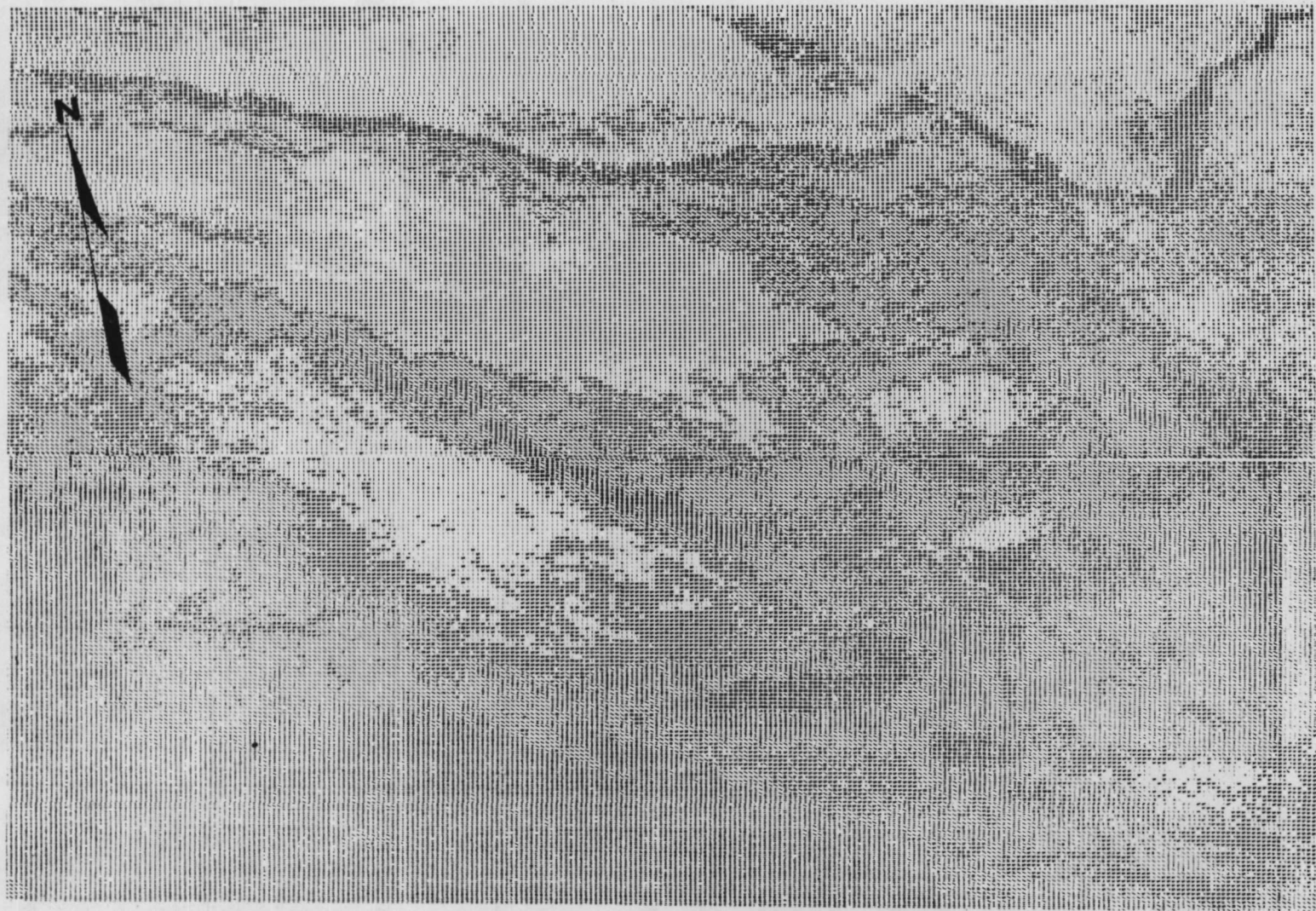
Figure 27. Segment of terrain map obtained by using simulations of ERTS 3-RBV camera data. Symbols used to designate the terrain classes are the same as in figure 25.
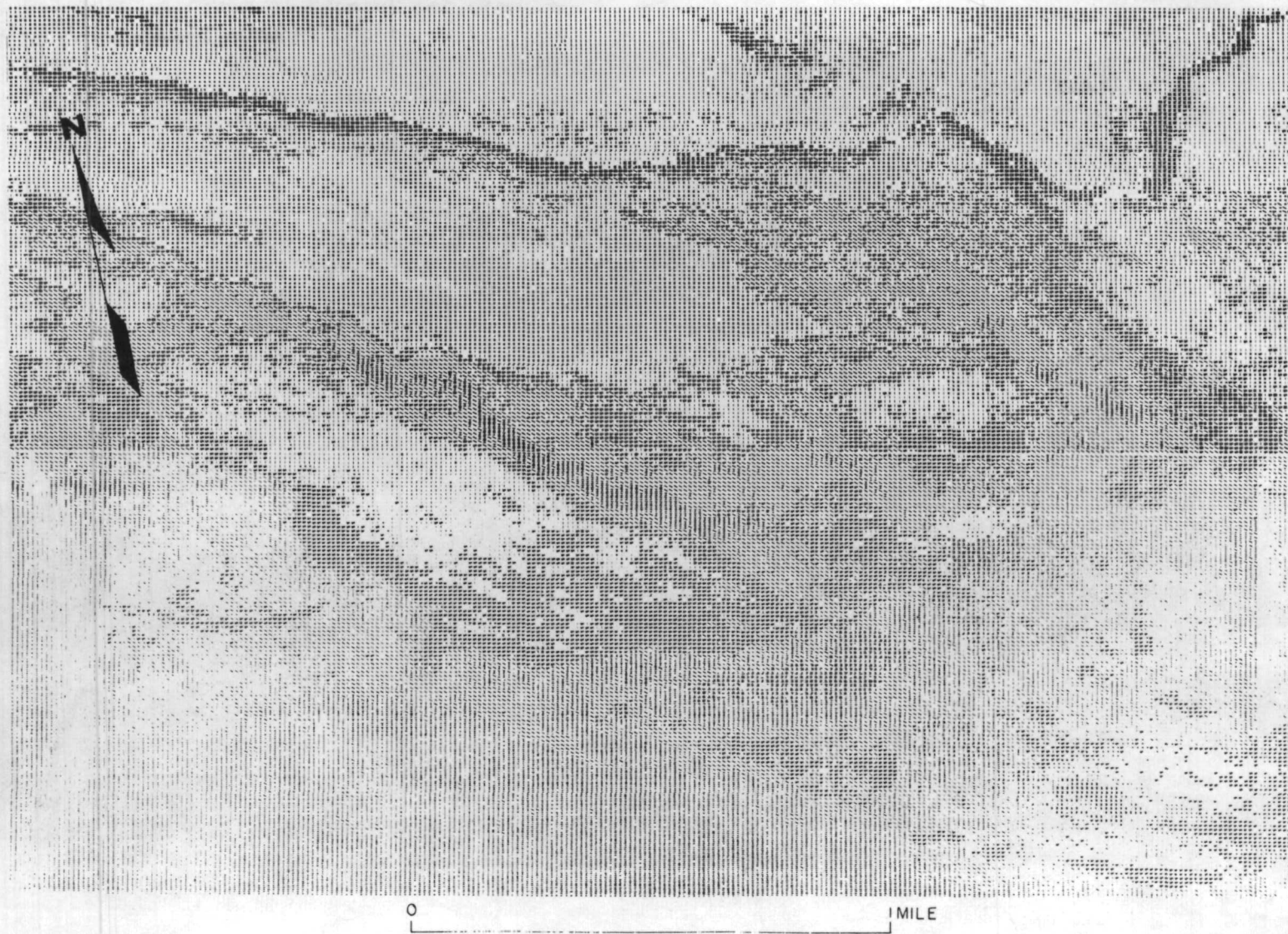
Figure 28. Segment of terrain map obtained by using simulation of ERTS 4-channel scanner data. Symbols used to designate the terrain classes are the same as in figure 25.
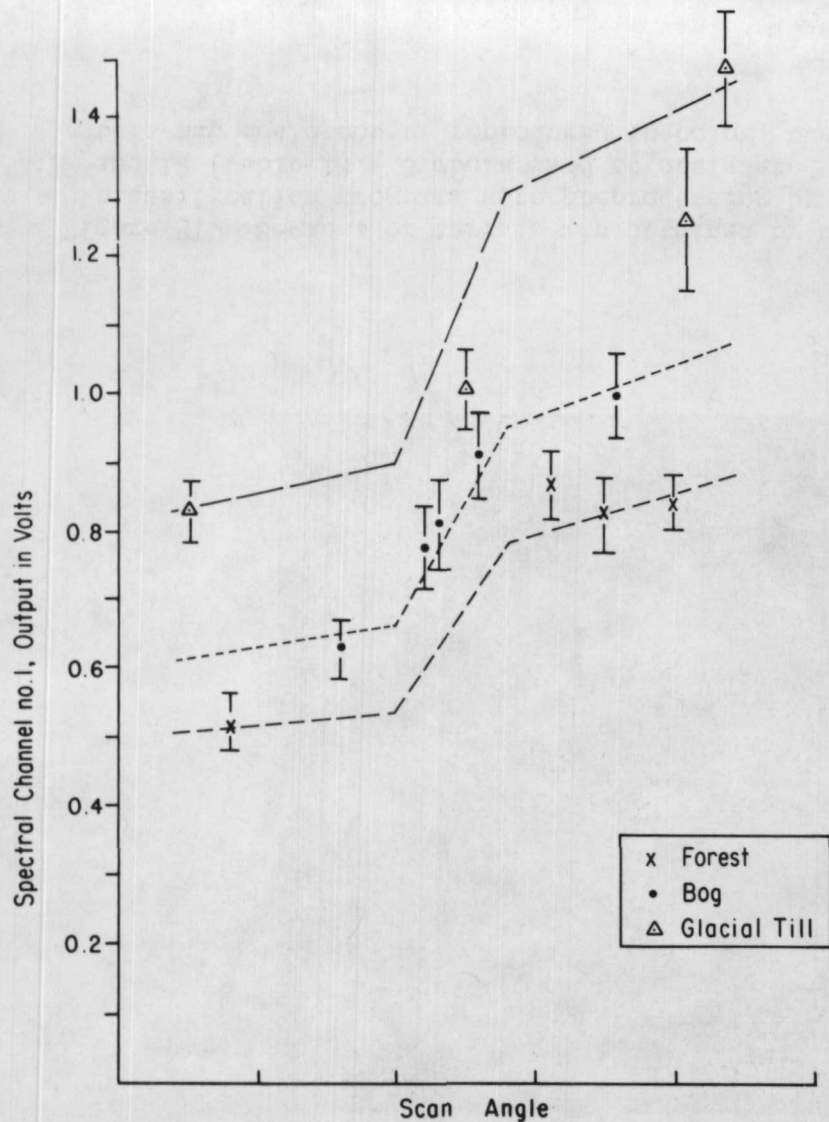
Figure 29. Spectral channel output versus scan angle for three classes, showing the scan angle functions. Each vertical bar is two standard deviations long, centered about the mean.
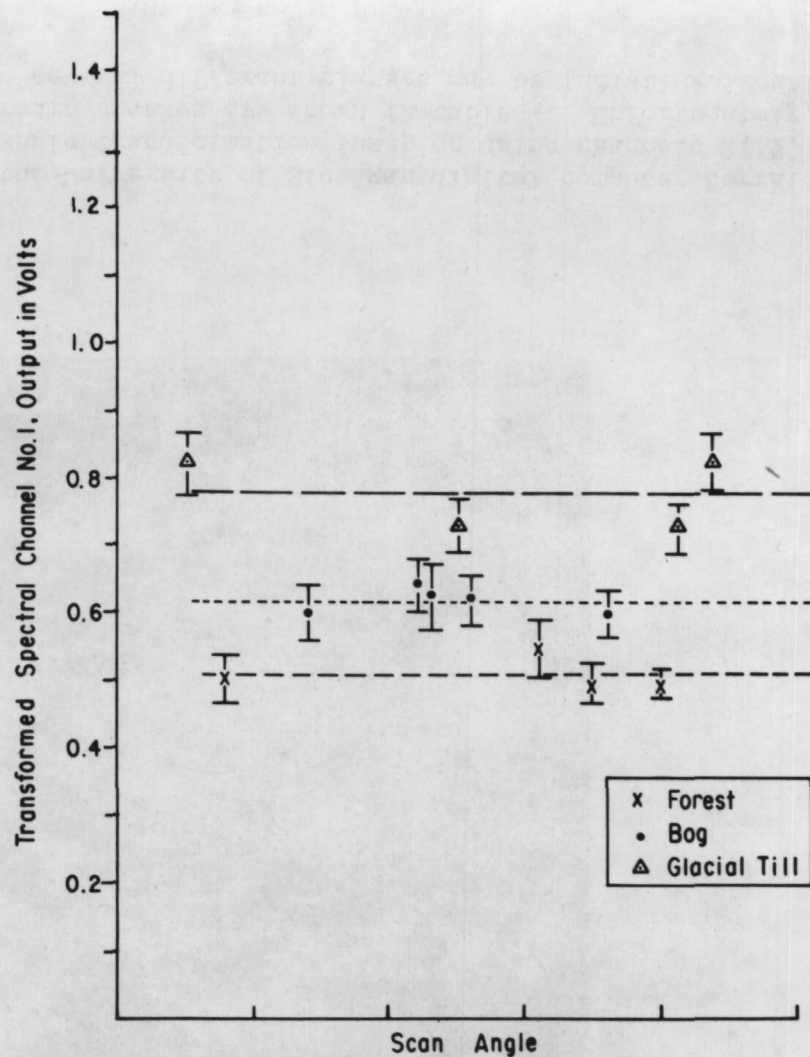
Figure 30. Transformed spectral channel output versus scan angle for three materials, showing mean values of combined (transformed) signatures. Each vertical bar is two standard deviations long, centered about the mean.

Figure 31.   Segment of terrain map obtained by using the University of Michigan digital computer terrain
    classification programs with preprocessing by scan-angle transformation function using channels 2, 5,
    and 12 (table 1).   Symbols used to designate the terrain classes are shown in table 4.   Unfortunately,
    this map could not be reproduced in color; therefore several different classes may be indistinguishable.
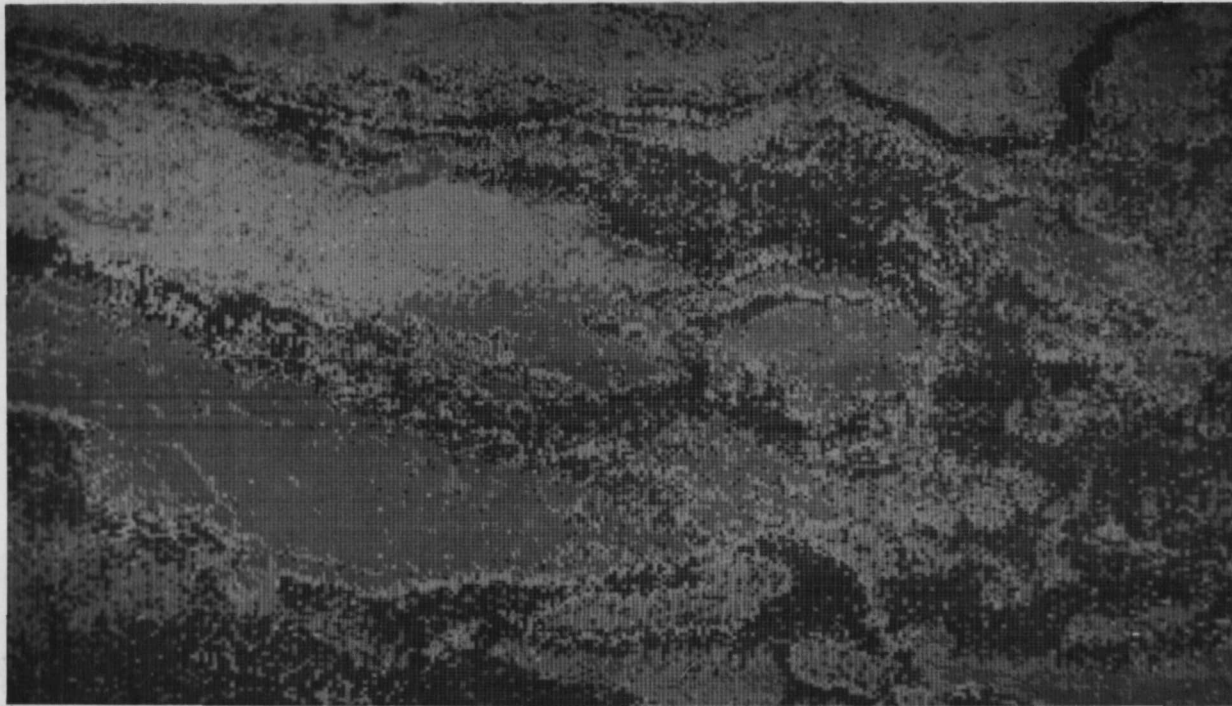
Figure 32. Segment of terrain map obtained by using the University of Michigan digital computer terrain classification programs with preprocessing by ratio transformation using simulated data of the ERTS 4-channel scanner. Symbols used to designate the terrain classes are shown in table 4.

Figure 33.   Computer-generated terrain map of entire test site, produced by University of Kansas
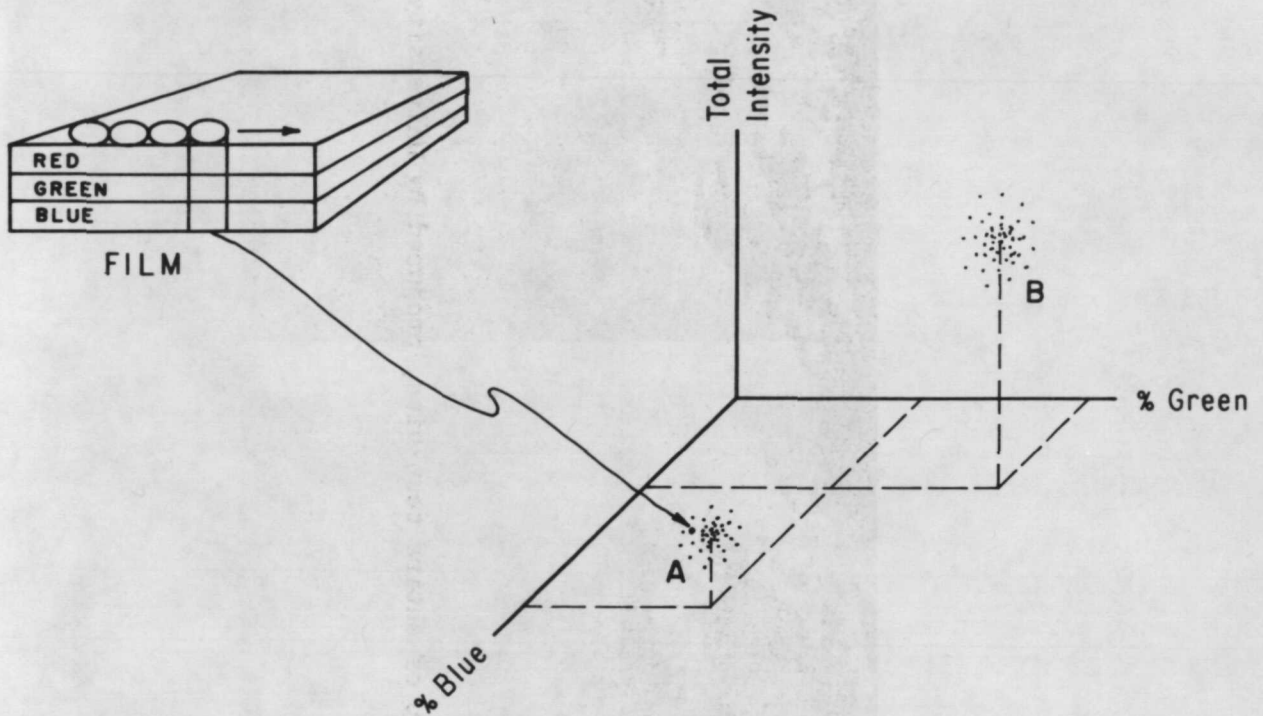   using spatial clustering techniques.

Figure 34. Schematic diagram showing scanning of color infrared aerial
film and the distribution of the density data from the three film
layers in three-color space. Four successive resolution cells along
the microdensitometer scan direction are shown. Hypothetical clusters
A and B represent two classes whose means have coordinates indicated
by the dashed lines. The arrow indicates the plotted position of
density data for one of the resolution cells, which falls within the
cluster of class A.

Figure 35. Black and white copy of color infrared aerial film used in
the clustering study (top image) showing two of the terrain classed
derived by computer processing as white circles (deciduous trees) and
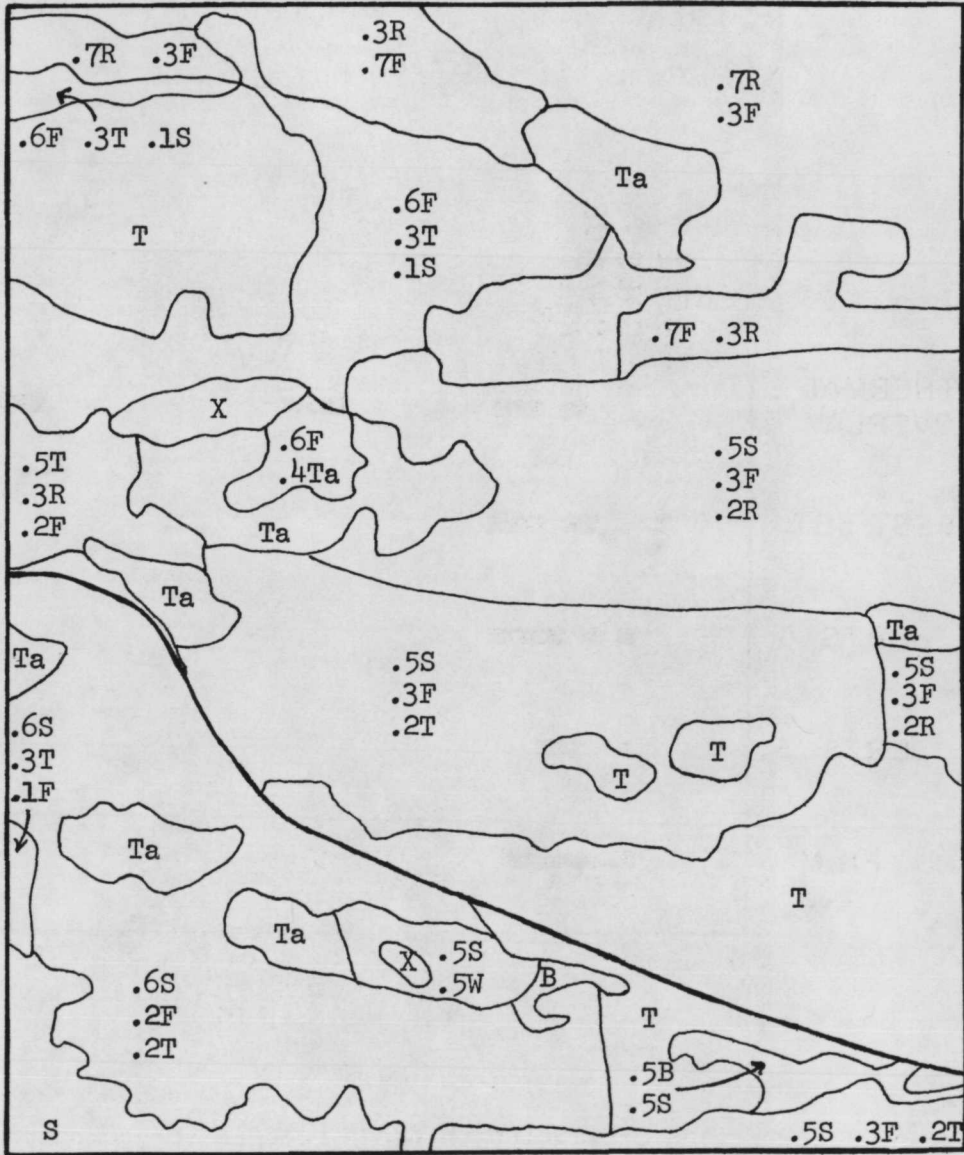squares (bedrock of basalt and amphibolite).

Figure 36. Segment of ground-control map, southeast corner of test site.

Numbers indicate decimal proportion of classes present in each outlined area. Classes are indicated by letters:

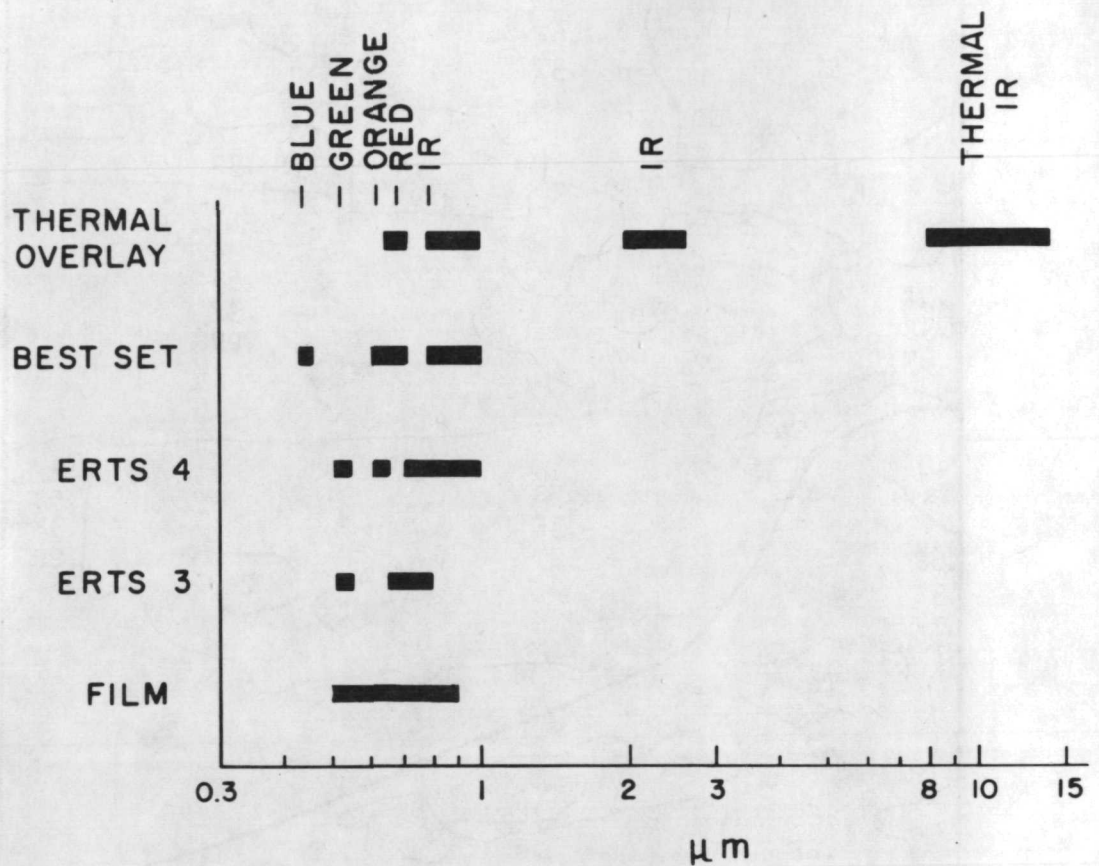|	
T	glacial till meadow
Ta	talus
F	forest
R	vegetated bedrock rubble
X	bedrock
W	water
S	shadow
B	Bog

The dark line is a road

Figure 37. Comparison of wavelength bands used in the computer studies.

THERMAL OVERLAY: four channels were combined and overlaid by the computer to make a single set of data from three scanner systems, using one reflective and two thermal scanners.

BEST SET: computer-selected best set of four reflective channels of data from the 12-channel scanner.

ERTS 4: simulation of the ERTS 4-channel scanner data.

ERTS 3: simulation of the ERTS 3 RBV camera data.

FILM: use of the three emulsion layers of color infrared film as a 3-band spectrometer for mapping by clustering techniques.